

5-31-2023

Biomechanical and psychophysical underpinnings of balance dysfunction in individuals with traumatic brain injury

Naphtaly Ehrenberg
New Jersey Institute of Technology

Follow this and additional works at: <https://digitalcommons.njit.edu/dissertations>



Part of the [Biomechanics Commons](#), [Biomedical Engineering and Bioengineering Commons](#), and the [Physiology Commons](#)

Recommended Citation

Ehrenberg, Naphtaly, "Biomechanical and psychophysical underpinnings of balance dysfunction in individuals with traumatic brain injury" (2023). *Dissertations*. 1661.
<https://digitalcommons.njit.edu/dissertations/1661>

This Dissertation is brought to you for free and open access by the Electronic Theses and Dissertations at Digital Commons @ NJIT. It has been accepted for inclusion in Dissertations by an authorized administrator of Digital Commons @ NJIT. For more information, please contact digitalcommons@njit.edu.

Copyright Warning & Restrictions

The copyright law of the United States (Title 17, United States Code) governs the making of photocopies or other reproductions of copyrighted material.

Under certain conditions specified in the law, libraries and archives are authorized to furnish a photocopy or other reproduction. One of these specified conditions is that the photocopy or reproduction is not to be “used for any purpose other than private study, scholarship, or research.” If a user makes a request for, or later uses, a photocopy or reproduction for purposes in excess of “fair use” that user may be liable for copyright infringement,

This institution reserves the right to refuse to accept a copying order if, in its judgment, fulfillment of the order would involve violation of copyright law.

Please Note: The author retains the copyright while the New Jersey Institute of Technology reserves the right to distribute this thesis or dissertation

Printing note: If you do not wish to print this page, then select “Pages from: first page # to: last page #” on the print dialog screen

The Van Houten library has removed some of the personal information and all signatures from the approval page and biographical sketches of theses and dissertations in order to protect the identity of NJIT graduates and faculty.

ABSTRACT

BIOMECHANICAL AND PSYCHOPHYSICAL UNDERPINNINGS OF BALANCE DYSFUNCTION IN INDIVIDUALS WITH TRAUMATIC BRAIN INJURY

**by
Naphtaly Ehrenberg**

Falls are a major burden on healthcare infrastructure, especially in older adults and even more so in older individuals that are living in institutions. According to data from the Centers for Disease Control and Prevention (CDC), from 2010 to 2020, unintentional falls were the leading cause of nonfatal emergency department visits for all age groups except among individuals from 15-24 years of age, where unintentional falls ranked a very close second to being unintentionally struck by or against. Among older individuals living in the community, approximately 30-35% fall at least once in a given year, and around three times as many falls over the same time period among adults living in institutions. Sustaining a fall can double an older individual's chances of sustaining a subsequent fall, and about one in five falls results in some kind of serious injury, such as a broken bone or head injury, with falls being the leading cause of traumatic brain injury (TBI).

Based on the CDC's 2014 data set, about 2.8 million people sustain a TBI in the United States every year, including over 837,000 children, contributing to over 56,000 deaths with over 2,500 of them being children. During this period, falls were the leading cause of TBI, accounting for approximately 48% of all TBI related emergency room (ER) visits, with older adults 65 and older and children ages 17 and below being most likely to suffer a TBI as a result of a fall, with falls being the cause in 49% and 81% of cases,

respectively. Depending on the exact nature and severity of a particular TBI, the resulting impairments can be both acute and long lasting, range from mild to debilitating, and can include sensory and perceptual deficiencies, reduced or altered cognitive function, and various types of motor deficits including paralysis, spasticity, and weakness. Balance dysfunction is a significant disabling factor post TBI, as it can increase the risk of falls which can in turn lead to subsequent brain injuries.

Postural control, the process of maintaining one's balance, is an essential ability that plays a crucial role in many everyday activities and is accomplished through the integration and coordination of visual, vestibular, proprioceptive inputs, and motor control to create a feedback system that maintains the body's center of mass (COM) above its' base of support. A TBI can affect postural control in multiple different ways, including direct damage to sensory processing regions responsible for handling essential balance related internal and external stimuli, or damaging motor control and planning areas that are responsible for generating appropriate muscular response to the above-mentioned stimuli. While damage to either of these cortical regions can lead to balance dysfunction, the specific regions effected, and the extent of the damage can necessitate different rehabilitation approaches when attempting to restore lost functionality. A loss or reduction of a particular sensory input or the ability to process that sensory input may require training an individual to shift their focus to the remaining sensory inputs, while the loss or reduction of motor control to a limb or joint would require the training of an individual to develop and utilize compensatory motor strategies for other limbs and joints to safely maintain their balance.

When standing quietly (or moving in an unperturbed fashion), an individual's postural control system only needs to account for internal changes resulting from the body's own movements, and the individual is more easily able to control the timing and intensity of required postural adjustments by limiting their movements to within the range of what their sensory and motor control systems can handle, i.e., if they have reduced muscle strength, perception, or reaction time, they can limit the speed or extent of their movements to make it easier for them to maintain their balance, rather than moving rapidly. However, when an individual's base of support is perturbed unexpectedly, their body needs to be able to determine and perform the necessary postural adjustments based on the perturbation that occurred, which can pose an increasing challenge depending upon the extent of injuries. Since they are less in control of the dynamics of the situation, their ability to perceive the perturbation is critical to their ability to adapt to it properly. The slower or less accurately they perceive the disturbance the less likely they are to be able to make the minimum postural adjustments needed to maintain stability, and the more likely they become to require exaggerated or significant postural adjustments that may be beyond their ability to safely perform. Since falls are a major concern, as mentioned above, and falls occur when the central nervous system fails to identify an impending loss of balance and or make the necessary adjustments to an individual's COM or base of support in time, an individual's ability to accurately perceive their environment during dynamic situations is critical to avoiding falls. Existing research that specifically quantifies impaired sensory integration in an objective manner post TBI is limited, and no prior work has investigated sensory acuity in individuals post TBI. While there are many well established methods for testing postural function that have been

validated in both healthy individuals and individuals with a variety of diagnoses, the evidence of these measures in association with balance interventions in individuals post TBI is sparse. To address this deficiency, this preliminary study employed a novel psychophysical approach to assess the perception of perturbation threshold of individuals post TBI and evaluate their kinematic and center of pressure (COP) behaviors during perturbed standing to attempt to detect differences in how individuals post TBI employ known balance control strategies.

**BIOMECHANICAL AND PSYCHOPHYSICAL UNDERPINNINGS OF
BALANCE DYSFUNCTION IN INDIVIDUALS WITH TRAUMATIC BRAIN
INJURY**

by
Naphtaly Ehrenberg

**A Dissertation
Submitted to the Faculty of
New Jersey Institute of Technology
and Rutgers University Biomedical and Health Sciences – Newark
in Partial Fulfillment of the Requirements for the Degree of
Doctor of Philosophy in Biomedical Engineering**

Department of Biomedical Engineering

May 2023

Copyright ©2023 by Naphtaly Ehrenberg

ALL RIGHTS RESERVED

APPROVAL PAGE

**BIOMECHANICAL AND PSYCHOPHYSICAL UNDERPINNINGS OF
BALANCE DYSFUNCTION IN INDIVIDUALS WITH TRAUMATIC BRAIN
INJURY**

Naphtaly Ehrenberg

Dr. Sergei Adamovich, Dissertation Co-Advisor Date
Professor of Biomedical Engineering, NJIT

Dr. Karen Nolan, Dissertation Co-Advisor Date
Associate Professor of Physical Medicine and Rehabilitation,
Rutgers University, Newark, NJ

Dr. Xianlian Zhou, Committee Member Date
Associate Professor of Biomedical Engineering, NJIT

Dr. Rakesh Pilkar, Committee Member Date
Associate Professor of Physical Medicine and Rehabilitation,
Rutgers University, Newark, NJ

Dr. Soha Saleh, Committee Member Date
Assistant Professor of Rehabilitation and Movement Sciences,
Rutgers University, Newark, NJ

BIOGRAPHICAL SKETCH

Author: Naphtaly Ehrenberg
Degree: Doctor of Philosophy
Date: May 2023

Undergraduate and Graduate Education:

- Doctor of Philosophy in Biomedical Engineering, New Jersey Institute of Technology, Newark, NJ, 2023 Rutgers University, Newark, NJ
- Master of Science in Biomedical Engineering, New Jersey Institute of Technology, Newark, NJ, 2011
- Bachelor of Science in Biomedical Engineering, New Jersey Institute of Technology, Newark, NJ, 2009

Major: Biomedical Engineering

Presentations and Publications:

Ehrenberg N, Veerubhotla A, Nolan K, Pilkar R. Balance Control Strategies during Perturbed Standing after a Traumatic Brain Injury: Kinematic Analysis. In: *2021 43rd Annual International Conference of the IEEE Engineering in Medicine and Biology Society (EMBC)*. IEEE; 2021:4855-4858. doi:10.1109/EMBC46164.2021.9630258

Veerubhotla A, Pilkar R, Ehrenberg N, Nolan K. J. Enhancing sensory acuity and balance function using near-sensory biofeedback-based perturbation intervention for individuals with traumatic brain injury. *NeuroRehabilitation*. 2021;48(1):29-37. doi:10.3233/NRE-201502

Pilkar R, Karunakaran K. K, Veerubhotla A, Ehrenberg N, Ibrionke O, Nolan K. J. Evaluating Sensory Acuity as a Marker of Balance Dysfunction After a Traumatic Brain Injury: A Psychophysical Approach. *Frontiers Neuroscience*. 2020;14. doi:10.3389/fnins.2020.00836

To my wife, my children, my family, my close friends, and anyone else who helped me
as I made my way through this convoluted journey.

Thank you.

To anyone who ever told me that I had the handwriting of a doctor:
you failed to specify the type of doctor.

“echuta”

“This is the way”

ACKNOWLEDGEMENT

I would like to express my sincere gratitude to my advisors, Dr. Sergei Adamovich, and Dr. Karen Nolan, for their encouragement, guidance, and support as I worked to complete my dissertation. I would also like to thank Dr. Rakesh Pilkar, Dr. Soha Saleh, and Dr. Xianlian Zhou for serving as my committee members.

I would like to extend a special thank you to Dr. Richard Foulds, Mr. John Hoinowski, and Mrs. Candida Rocha for their support during the early years of my doctoral work, and I would also like to thank all of my former lab members at NJIT, Drs. Ghaith Androwis, Kevin Abbruzzese, Madeline Corrigan, Kiran Karunakaran, Peter Michael, and Darnell Simon for their support, feedback, and camaraderie during the time that we spent together.

I would like to thank my colleagues at the Kessler Foundation for their support and encouragement during the later years of my doctoral work, with a very special thank you once again to Dr. Kiran Karunakaran for her continued support and assistance.

I would like to thank Dr. Naftali Wein, my very close friend, his mother Mrs. Hindi Wein, and the late Rabbi Moshe Wein ז"ל, for all their support and encouragement throughout life's many ups and downs over the years.

I would like to thank my family for their encouragement and support during my doctoral work, and lastly, I would like to thank my wife Rachie for her understanding, support, and encouragement throughout this longer than expected journey.

TABLE OF CONTENTS

Chapter	Page
1 INTRODUCTION.....	1
1.1 Background and Significance of Traumatic Brain Injury.....	1
1.2 Balance – What is Involved and How Does It Work.....	5
1.3 Balance Control Strategies.....	8
1.4 Falls – Prevalence, Causes, and Resulting Complications of Falls.....	13
1.5 Literature Gap – Limited Evidence of Balance Measures in TBI.....	13
2 METHODS.....	14
2.1 Research Aims.....	14
2.2 Research Participants.....	16
2.3 Instrumentation and Experimental Setup.....	17
2.4 Data Collection Procedures for Research Assessments.....	30
2.5 Clinical Assessments.....	33
2.6 Data Processing.....	34
2.7 Statistical Analysis.....	35
3 EVALUATING SENSORY ACUITY AFTER A TBI.....	36
3.1 Methods and Results.....	36
4 KINEMATIC ANALYSIS OF PERTURBED STNADING AFTER A TBI: A PILOT STUDY.....	39
4.1 Methods and Results.....	39
5 RESULTS.....	44
5.1 Functional Assessments.....	44

TABLE OF CONTENTS
(Continued)

5.2 Sensory Acuity Measure.....	45
5.3 Kinematic Measures.....	46
5.4 Correlations Between Kinematic and Functional Measures	76
6 DISCUSSION.....	78
6.1 General Discussion.....	78
6.2 Limitations.....	81
6.3 Future Directions.....	81
REFERENCES.....	84

LIST OF TABLES

Table		Page
1.1	Classification of TBI Severity	2
2.1	Number of Participants by Group	17
4.1	Demographics and Functional Assessments.....	42
5.1	Participant Demographics and Functional Assessments.....	45
5.2	Perceived Perturbation Threshold by Perturbation Frequency.....	46

LIST OF FIGURES

Figure		Page
1.1	Locations and lines of action of the muscles required to maintain balance in the sagittal plane	9
1.2	Sagittal plane balance strategies.....	10
2.1	Calibration frame configuration.....	20
2.2	Kessler Helen Hayes markerset for balance lab	23
2.3	Experimental setup for Standard Trials Assessment	31
2.4	Amplitude iteration and Psychometric Curve	32
2.5	Simplified experimental setup for PPT Assessment.....	33
4.1	Mean range and RMS values for hip, knee, and ankle joints for HC and TBI groups.....	43
5.1	Hip Joint Angle Range - 0.33Hz Standard Trials.....	48
5.2	Knee Joint Angle Range - 0.33Hz Standard Trials.....	49
5.3	Ankle Joint Angle Range - 0.33Hz Standard Trials.....	50
5.4	COM AP-ML Path Length - 0.33Hz Standard Trials.....	51
5.5	COM AP-ML Average Velocity - 0.33Hz Standard Trials.....	52
5.6	COM AP Range - 0.33Hz Standard Trials.....	54
5.7	COP AP-ML Path Length - 0.33Hz Standard Trials.....	55
5.8	COP AP-ML Average Velocity - 0.33Hz Standard Trials.....	56
5.9	COP AP Range - 0.33Hz Standard Trials.....	57
5.10	Hip Joint Angle Range - 0.5Hz Standard Trials.....	58
5.11	Knee Joint Angle Range - 0.5Hz Standard Trials.....	59
5.12	Ankle Joint Angle Range - 0.5Hz Standard Trials.....	60

**LIST OF FIGURES
(Continued)**

5.13	COM AP-ML Path Length - 0.5Hz Standard Trials.....	61
5.14	COM AP-ML Average Velocity - 0.5Hz Standard Trials.....	62
5.15	COM AP Range - 0.5Hz Standard Trials.....	63
5.16	COP AP-ML Path Length - 0.5Hz Standard Trials.....	64
5.17	COP AP-ML Average Velocity - 0.5Hz Standard Trials.....	65
5.18	COP AP Range - 0.5Hz Standard Trials.....	66
5.19	Hip Joint Angle Range – 1.0Hz Standard Trials.....	68
5.20	Knee Joint Angle Range - 1.0Hz Standard Trials.....	69
5.21	Ankle Joint Angle Range - 1.0Hz Standard Trials.....	70
5.22	COM AP-ML Path Length - 1.0Hz Standard Trials.....	71
5.23	COM AP-ML Average Velocity - 1.0Hz Standard Trials.....	72
5.24	COM AP Range - 1.0Hz Standard Trials.....	73
5.25	COP AP-ML Path Length - 1.0Hz Standard Trials.....	74
5.26	COP AP-ML Average Velocity - 1.0Hz Standard Trials.....	75
5.27	COP AP Range - 1.0Hz Standard Trials.....	76

CHAPTER 1

INTRODUCTION

1.1 Background and Significance of Traumatic Brain Injury

According to the Centers for Disease Control and Prevention (CDC), a traumatic brain injury (TBI) can be caused by a bump, blow or jolt to the head or a penetrating head injury that disrupts normal brain function. Based on the CDC's 2014 data set, about 2.8 million people sustain a TBI in the United States every year, including over 837,000 in children, contributing to over 56,000 deaths with over 2,500 of them being children. During this period, falls were the leading cause of TBI, accounting for approximately 48% of all TBI related emergency room (ER) visits, with older adults 65 and older and children ages 17 and below being most likely to suffer a TBI as a result of a fall, with falls being the cause in 49% and 81% of cases, respectively. The second most prevalent cause of TBI related ER visits was being struck by or against an object, which occurred in approximately 17% of overall cases in the US and accounted for approximately 28% of cases in children 17 and under [1].

TBIs are classified by the type(s) of the injuries sustained; primary vs secondary, focal vs diffuse, and penetrating vs non-penetrating, and the severity of the injury; mild, moderate, or severe. Primary injuries are sudden injuries that are mechanically induced at the time of impact, and include various types bruising, bleeding, and skull fractures, while secondary injuries are metabolic and physiological irregularities that may begin at the time of injury and last for an extended period of time or have a delayed onset sometime after the injury occurs [1]–[3]. Focal injuries are limited to a particular area of

the brain and are usually caused by contact as a result of linear acceleration and deceleration, including scalp injuries, skull fractures, and brain contusions, while diffuse injuries affect larger and or multiple areas of the brain and are caused by twisting and shearing forces [2], [3]. Penetrating injuries are when the skull and dura mater are compromised as a result of trauma, and non-penetrating injuries are when the skull and dura mater remain intact after sustaining trauma [2], [3].

The acute severity of a TBI is determined at the time of injury and is categorized as mild, moderate, or severe, based on the duration of three physiological criterion in the aftermath of the trauma sustained including loss of consciousness (LOC), alterations of consciousness (AOC), and post-traumatic amnesia (PTA) as shown in Table 1.1. In the event that it is not clinically possible to determine severity in this fashion due to a medically induced coma or other confounding factor, other measures are used to assess severity, including medical imaging and the Glasgow Coma Scale (GCS). If an individual presents with symptoms that match more than one severity category, the higher severity is applied, though 70-90% of all TBIs are classified as mild [4], [5].

Table 1.1. Classification of TBI Severity [4]

Criteria	Mild	Moderate	Severe
Structural Image	Normal	Normal or Abnormal	Normal or Abnormal
Loss of Consciousness (LOC)	0-30 min	> 30 min and < 24 hrs.	> 24 hrs.
Alteration of Consciousness (AOC)	A moment up to 24 hrs.	> 24 hrs. Severity bases on other criteria	
Post-Traumatic Amnesia	0-1 Day	> 1 Day and < 7 Days	> 7 Days
Glasgow Coma Scale	13-15	9-12	< 9

Depending on the exact nature and severity of a particular TBI, the resulting impairments can be both acute and long lasting, range from mild to debilitating, and can include sensory and perceptual deficiencies, reduced or altered cognitive function, and various types of motor deficits including paralysis, spasticity, and weakness [6]. Balance dysfunction is a significant disabling factor post TBI, as it can increase the risk of falls which can in turn lead to subsequent brain injuries and is reported in between 30-65% of cases of TBI. Aside from the risk of further injury associated with balance dysfunction, it can also have a significant effect on an individual's quality of life and ability to live independently, as it is fundamentally involved in a large number of activities of daily living, including sitting, standing, walking, and self-care [7].

Postural control, the process of maintaining one's balance, is an essential ability that plays a crucial role in many everyday activities and is accomplished through the integration and coordination of visual, vestibular, proprioceptive inputs, and motor control to create a feedback system that maintains the body's center of mass (COM) within its' base of support. Postural control can be both subconscious and conscious, with normal body sway being an example of subconscious postural control and standing on one foot being an example of conscious postural control. A TBI can affect postural control in multiple different ways, including direct damage to sensory processing regions responsible for handling essential balance related internal and external stimuli, or damaging motor control and planning areas that are responsible for generating appropriate muscular responses to the above-mentioned stimuli. While damage to either of these cortical regions can lead to balance dysfunction, the specific regions effected, and the extent of the damage can necessitate different rehabilitation approaches when

attempting to restore lost functionality. A loss or reduction of a particular sensory input or the ability to process that sensory input may require training an individual to shift their focus to the remaining sensory inputs, while the loss or reduction of motor control to a limb or joint would require the training of an individual to develop and utilize compensatory motor strategies for other limbs and joints to safely maintain their balance.

When standing quietly (or moving in an unperturbed fashion), an individual's postural control system only needs to account for internal changes resulting from the body's own movements, and the individual is more easily able to control the timing and intensity of required postural adjustments by limiting their movements to within the range of what their sensory and motor control systems can handle, i.e., if they have reduced muscle strength, perception, or reaction time, they can limit the speed or length of their steps to make it easier for them to maintain their balance, rather than running. However, when an individual's base of support is perturbed unexpectedly, their body needs to be able to determine and perform the necessary postural adjustments based on the perturbation that occurred, which can pose an increasing challenge depending upon the extent of injuries. Since they are less in control of the dynamics of the situation, their ability to perceive the perturbation is critical to their ability to adapt to it properly. The slower or less accurately they perceive the disturbance the less likely they are to be able to make the minimum postural adjustments needed to maintain stability, and the more likely they become to require exaggerated or significant postural adjustments that may be beyond their ability to safely perform.

Two commonly used clinical assessments for determining the presence of balance dysfunction are the Berg Balance Scale (BBS), and the Dynamic Gait Index (DGI), and

while these assessments can be useful for quantifying an individual's global ability to maintain their balance during common activities, they do not quantify the underlying cause(s) of dysfunction. Since falls are a major concern, as mentioned above, and falls occur when the central nervous system fails to identify an impending loss of balance and or make the necessary adjustments to an individual's COM or base of support in time, an individual's ability to accurately perceive their environment during dynamic situations is critical to avoiding falls. Existing research that specifically quantifies impaired sensory integration in an objective manner post TBI is limited [8], and no prior work has investigated sensory acuity in individuals post TBI. To address this gap in the literature, the preliminary study presented below employed a novel psychophysical approach to assess perception of perturbation threshold and evaluate the efficacy of a biofeedback intervention intended to lower the detection threshold in individuals post TBI, with further analysis of kinematic and center of pressure (COP) data being performed to better understand the biomechanical and psychophysical underpinnings of balance dysfunction in individuals post TBI.

1.2 Balance – What is Involved and How Does it Work

Balance is the process by which an individual maintains their center of mass above their base of support to resist the effects of gravity and remain upright. Sensory information used by the brain to maintain balance comes from three sources, vision, proprioception, and the vestibular system [9]. Binocular vision allows humans to perceive the distance between objects in their environment as well as their relative movements. Vision plays an important role in balance, as aside from giving the brain information about the

surrounding environment, it can also give the brain information about how the body is moving relative to the environment, even if the body itself is not actively causing that movement. This visual information can supplement inputs from other sensory sources but can also provide information that they cannot detect [10].

The human vestibular system is located within the inner ears, and contains two main structures, the Otolith Organs, and the Semicircular Canals. The Otolith Organs are a pair of structures within the inner ear called the sacculus and the utricle, that contain sensory hairs that extended into a viscous layer that is covered by membrane structure that contains calcium carbonate crystals. These crystals make the membrane denser than the rest of the surrounding structure, and enable motions of the head that result in a shearing movement of the membrane relative to the sensory hairs to be detected. To facilitate the detection of linear acceleration and displacement of the head regardless of the direction of movement, the sacculus is oriented vertically to respond to up and down, and anterior and posterior movements in the sagittal plane, and the utricle is oriented horizontally to respond to lateral head movements and sideways tilts in the horizontal plane. The Semicircular Canals are made up of three mutually perpendicular canals filled with endolymph fluid that are responsible for detecting head rotation resulting from angular accelerations. Each canal features a bulbous area at its base called the ampulla which in turn contains the cupula, a gelatinous mass that contains sensory hairs. The cupula extends from its base to fill the entire cross section of the ampulla, forming a barrier that prevents the passage of endolymph fluid. When movement occurs along the plane of one of the canals, the inertia of the endolymph displaces the cupula from its resting position in the opposite direction of the movement and this shift is detected by the

sensory hairs and causes the associated neurons to modulate their firing rate. Canals in the same plane that are located on opposite sides of the head work in tandem, with the canal on the leading side of the direction of movement increasing its firing rate and the opposite canal reducing its firing rate. This is due to difference in the direction of the flow of the endolymph fluid between the two canals, and this differential firing enables the Semicircular Canals to detect rotations that occur in any direction [11].

Proprioception is the body's sense of where the limbs are positioned in space and how they are moving and is independent of the visual and vestibular systems.

Proprioceptive sensory information is detected by receptors located within the body's skeletal muscles, joints, and skin via muscle spindles, Golgi tendon organs, and cutaneous mechanoreceptors. Muscle spindles are mechanoreceptors that are located in parallel with skeletal muscles, are often considered the primary receptors supplying the body's sense of proprioception, and are sensitive to the length of a given muscle and changes in that muscles length, enabling awareness of the configuration of even non-contracting muscles. Golgi tendon organs are located in series with skeletal muscles and are situated at the interface between muscle fibers and tendons. Golgi tendon organs are sensitive to the development of tension in the surrounding tissue, enabling the monitoring of the force generated by contracting muscles. Cutaneous mechanoreceptors located near joints can sense skin stretching that result from movement, while similar receptors elsewhere on the skin sense inter limb and environmental contact and interaction to round out the body's internal sense of its configuration [12].

1.3 Balance Control Strategies

In their 1985 paper, *The organization of human postural movements: A formal basis and experimental synthesis*, Nasher & McCollum presented an approach for understanding human postural control in the sagittal plane that took into account the geometric and mechanical properties of human movement and applied some hypothesized neurological limits in an effort to characterize the muscle activations and movement trajectories that are the basis for making postural adjustments while standing. The limits that they worked under were that the postural responses should use the minimum number of muscles needed to correct instability, and that frequently utilized postural adjustments are organized to minimize the neurological load of decision making.

While standing fully erect, the body is only stable with the center of mass directly above the geometric center of its base of support, as any deviation from this precise configuration will result in the force of gravity further increasing the magnitude of the deviation. Stability can be regained via postural adjustments that exert the necessary stabilizing forces against the support surface needed to properly reposition the center of mass, and these adjustments can be made via many possible combinations of leg and trunk muscle activation about the hip, knee, and ankle. For the purpose of their approach, Nasher & McCollum set the minimum number of muscles required to control the configuration of these three joints in the sagittal plane at six, with an antagonistic pair of muscles acting around each joint, specifically, the tibialis anterior and gastrocnemius for ankle plantarflexion and dorsiflexion, respectively, the gastrocnemius and hamstrings for knee flexion and the quadriceps for knee extension, and the quadriceps and abdominals for hip extension and the hamstrings and paraspinals for hip extension (see Figure 1.1)

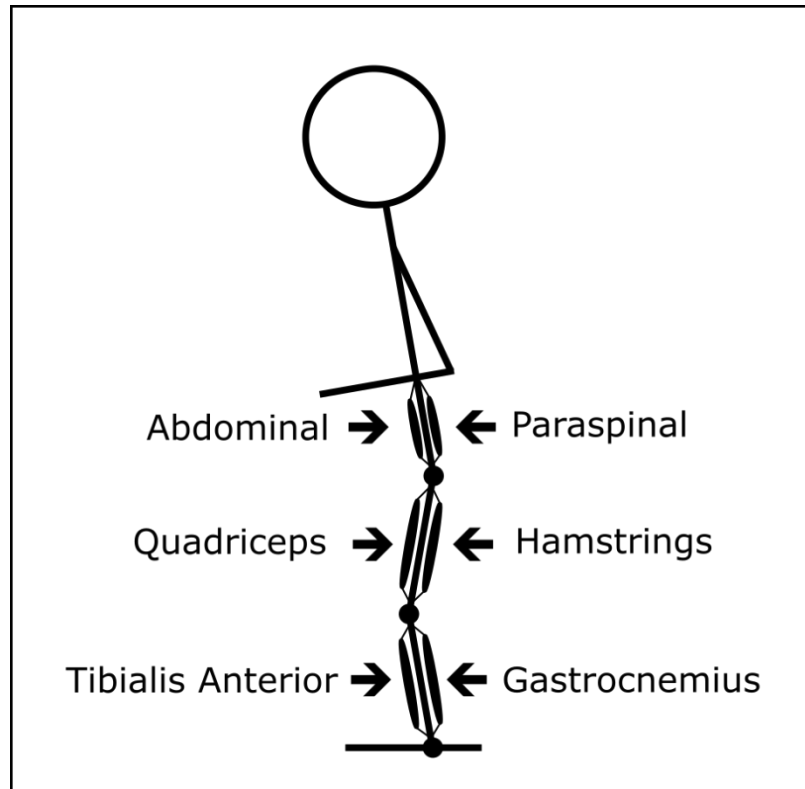


Figure 1.1. Simplified locations and lines of action of the muscles required to maintain balance in the sagittal plane.

When healthy individuals are subjected to perturbation in the anterior-posterior direction while standing, they employ stereotypical muscle activation patterns to maintain their balance that Nasher & McCollum referred to as muscle synergies, and these synergies predominantly involved motion about the ankle and hip joints while keeping the knee fully extended, so Nasher & McCollum focused their analysis on ankle and hip motion and fully erect standing.

While standing, Nasher & McCollum describe the behavior of participants subjected to perturbations as employing a pure ankle strategy, a pure hip strategy, or a sequential mixture of ankle and hip strategies (see Figure 1.2). A pure ankle strategy consists of net muscle torque being generated to induce movement about the ankle to counter the movement of the COM in response to the perturbation. This occurs via

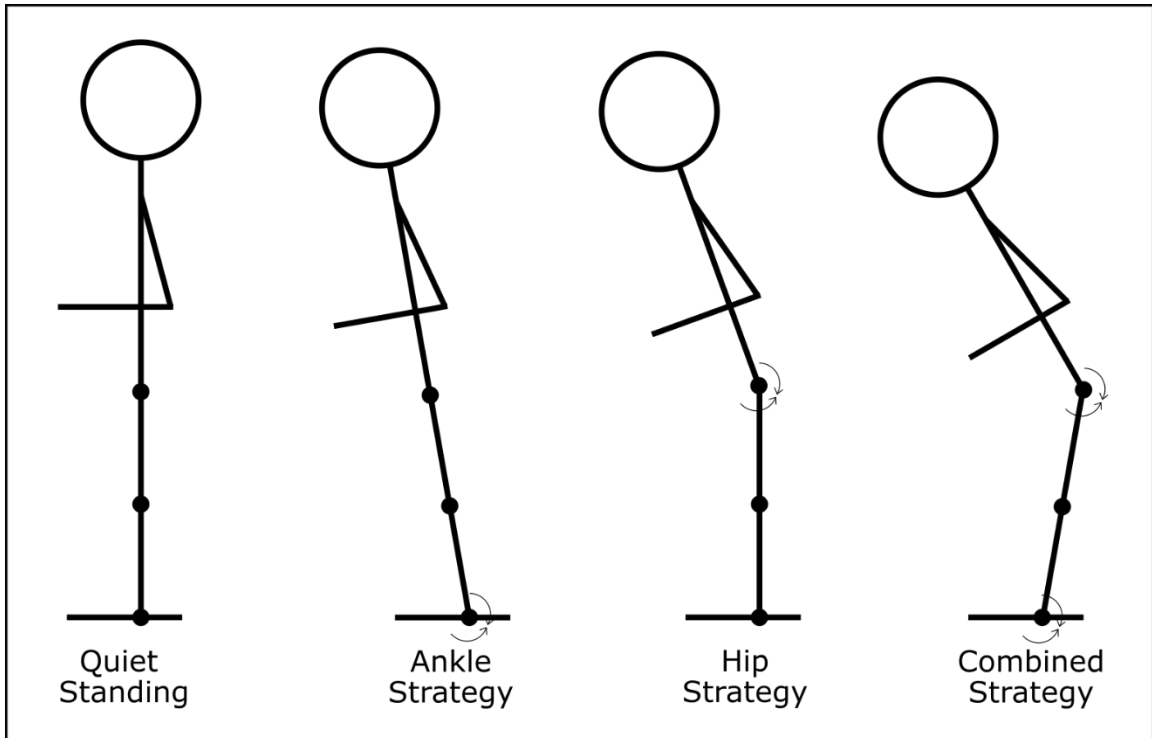


Figure 1.2. Sagittal plane balance strategies with the location of net torque indicated.

dorsiflexion or plantarflexion depending on the direction of the perturbation, while only stabilizing muscle activity is generated about the hip and knee to maintain the relative position of the other bodies segments, so no movement occurs about those joints, and was commonly employed by participants when the support surface was larger than the size of their foot. Conversely when the size of the support surface was reduce to significantly shorter than their foot, most participants employed a pure hip strategy which consists of net muscle torque being generated to induce movement about the hip to counter the movement of the COM in response to the perturbation, via flexion or extension depending on the direction of the perturbation, but in this case the ankle moves passively in the opposite direction of the hips and only the knee is held fixed. The remaining participants employed a sequential mixture and ankle and hip strategies, though this approach proved to be much less successful, as many of those participants failed to

maintain their balance in response to the applied perturbations. Reducing the size of the support surface served as a method to restrict the amount of torque that could be generated about the ankle, which according to Nasher & McCollum appeared to be the main driver in causing participants to switch from a pure ankle to a pure hip, or mixed, strategy [9].

A later work by Horak & Nasher in 1986 discussed the above introduced balance strategies directly and comprehensively. They describe the ankle strategy as a muscle activation sequence starting about the ankle joint that then progressed proximally to the thigh and then the trunk muscles. The muscle activations associated with this strategy all occur along the either the dorsal or ventral surface of the body, depending on the direction of the applied perturbation, and the postural correction movement took place predominantly about the ankle joint, hence the term ankle strategy. However, this occurred when the support surface was sufficiently large, as a different response was once again observed on support surface shorter than the foot. In that situation, they describe the hip strategy as consisting of similarly timed muscle activations to the ankle strategy but occurring in a different configuration. Not only do the muscles activate in a distal progression starting with the trunk muscles and then proceeding to the thigh muscles, but the muscle activations occur on the opposite side of the body compared to the ankle strategy for a given perturbation, with generally no activation about the ankle. The use of an intermediately sized support surface, as well as switching back and forth between various sized support surfaced demonstrated that ankle and hip strategies could be combined in a virtually limitless number of ways by varying the timing and scale of the components used [13].

A few years Nasher, Shupert, and Horak further characterized the aforementioned postural control strategies by analyzing the mechanical and sensory limitations of each strategy. The ankle strategy is capable of handling up to approximately 12 degrees of COM sway in the AP direction, but only at low frequencies up to approximately 1 Hz, due to the large moment of inertia of the rest of the body acting about the ankle. The ankle strategy is limited to this range not because of a lack of strength in the ankle muscles, as the forces generated by these same muscles during other activities are far larger, but because of the maximum torque that these muscles can generate about the ankle joint, which is limited by the size of the feet compared to the body's mass and height. Conversely, the hip strategy applies torque about the hips to move both the hip and ankle joints to alter the position of the COM, and while it can execute these movements very quickly in the range of approximately 0.5 – 2.5 Hz, it is only able to handle approximately 3 degrees of sway, and cannot maintain leaning in the AP direction as the torques used rely on the transient inertia of the segments involved which cannot compensate for gravity at low frequencies, and are limited by the strength of the muscles acting about the hip joint relative to the inertial properties of the body at higher frequencies. The ankle and hip strategies can be combined in a variety of ways due to the fact that the movements of the hip strategy are effective over the whole range of the limits of stability of the ankle, and because the two strategies can operate at different frequencies, the hip strategies 3 degrees of additional sway control can be employed at any point within the 12 degrees limits of stability of ankle sway [14]. The three postural control strategies articulated in these initial works, the ankle strategy, the hip strategy,

and the combined strategy, continued to be used as the foundation for further study of human balance control [15] and are still in use today [16].

1.4 Falls – Prevalence, Causes, and Resulting Complications of Falls

Falls are a major burden on healthcare infrastructure, especially in older adults and even more so in older individuals that are living in institutions [17], [18]. According to data from the CDC, from 2010 to 2020, unintentional falls were the leading cause of nonfatal emergency department visits for all age groups except among those from 15-24 years of age, where unintentional falls ranked a very close second to being unintentional struck by or against [19]. Among older individuals living the community, approximately 30-35% fall at least once in a given year, and around three times as many falls over the same time period among adults living in institutions [17], [18]. Sustaining a fall can double an older individual's chances of sustaining a subsequent fall, and about one in five falls results in some kind of serious injury, such as a broken bone or head injury, with falls being the leading cause of TBI [18].

1.5 Literature Gap – Limited Evidence of Balance Measures in TBI

There are many well establish methods for testing postural function that have been validated in both healthy individuals and individuals with a variety of diagnoses, include COP metrics such as RMS, velocity, and path length, and kinematic metrics using similar measures applied to the COM rather than the COP [20]. However, the evidence of these measures in association with balance interventions in individuals post TBI is sparse [21], and the present study provides an ideal opportunity to work towards filling this gap.

CHAPTER 2

METHODS

2.1 Research Aims

Postural Control Strategies after TBI

Aim 1: To investigate postural control strategies and their relationship to sensory acuity in perturbed standing in individuals post TBI compared to healthy controls.

Hypothesis 1A: Individuals post TBI will shift from an **ankle strategy** to a **hip/mixed strategy** at **lower perturbation amplitudes** compared to healthy participants.

Hypothesis 1B: The **higher an individual's PPT** at a given frequency (meaning their sensitivity is lower/ their ability to detect perturbations is lower/poorer so they can only detect larger perturbations), the **lower the amplitude** that their **postural control strategy** will shift from ankle to hip/mixed.

Aim 1 Outcome Measures:

Postural Control Strategies: The directionality and velocity of ankle/lower limb and trunk COM excursions, and the amplitude, velocity, and spectral components of ankle, knee, and trunk joint angles will be used to identify what strategies were used for a given condition [9].

Perception of Perturbation Threshold (PPT): SIAM will be used to assess participant's perception thresholds at each perturbation frequency, both before and after the CBB intervention [22].

Kinematic Indices after TBI

Aim 2: To preliminarily assess the sensitivity and validity of kinematic metrics of balance dysfunction during perturbed standing in individuals post TBI compared to healthy controls.

Hypothesis 2A: **Kinematic balance metrics**, including COM RMS, COM velocity, etc. will show clear signs of **instability** in individuals post TBI, with the **instability increasing** along with the **difficulty of the balance task**.

Aim 2 Outcome Measures:

Kinematic Assessments of Balance: Optical motion capture data will be used to calculate center of mass (COM) data in 3 dimensions for the entire body as well as various combinations of limb segments using Cortex. This will then enable several COM metrics to be measured, including but not limited to: RMS, standard deviation, velocity, path length, and spectral composition.

Clinical Assessments of Balance: The Berg Balance Scale (BBS), 10 Meter Walk Test, 5 Meter Walk Test, and Timed up and Go test will be used to clinically assess balance dysfunction [20], [22], [23].

Kinematics, COP, and Sensory Acuity Correlations after TBI

Aim 3: To identify correlates and interdependencies among kinematic indices, COP metrics, and sensory acuity during perturbed standing in individuals post TBI compared to healthy controls.

Hypothesis 3A: **Kinematic and COP metrics of stability**, including RMS, velocity, etc., and **sensory acuity** will show **negative correlations** with improvements in **clinical assessments**.

Aim 3 Outcome Measures:

Quantitative Analysis of Postural Control: Postural control variables enumerated by Pallard, T. et al in his 2015 review article that can be reliably extracted from the available data sources within this study will be compared to identify relationships and interdependencies that are relevant to balance dysfunction in perturbed standing in individuals post TBI [20].

2.2 Research Participants

Nine healthy individuals with no existing orthopedic, neurological or visual impairments were recruited for the study to serve as healthy controls (HC) along with twelve TBI participants with varying levels of impairment (Table 2.1). Inclusion criterion for the TBI participants were: 1) between 18 and 60 years of age, 2) diagnosed with a non-penetrating TBI six or more months prior, 3) able to stand unsupported for at least five minutes, 4) willing and able to give informed consent. Exclusion criteria for the TBI participants were: 1) a history of injury to the lower limbs within the past ninety days, 2) cardiac disease, 3) a previous history of balance impairment prior to their TBI. All study related procedures were approved by the Kessler Foundation IRB, and informed consent was obtained from all participants prior to participating in any study related activities.

Ten additional subjects participated in the study, but their data was excluded for various reasons. Six HC participants were removed from the dataset; two were excluded

for excessive voluntary sway and another two were excluded due to missing motion capture markers, and of the remaining two, one was excluded due to being distracted and talking during data collection, and the other was excluded due to not completing the study. Four TBI participants were also removed from the dataset; one was excluded due to excessive movement caused by their loss of balance, another was excluded due to excessive movement caused by their near loss of balance and subsequent overcompensation, an additional participant was excluded as a result of outlier analysis, and the final participant was excluded due to not completing the study.

Table 2.1 Number of Participants by Group

Group	Number of Participants
Health Control	9
TBI	12

2.3 Instrumentation and Experimental Setup

Optical Motion Capture System

A Motion Analysis Corporation (MAC, Santa Rosa, CA) passive optical motion capture system was used to record the 3-dimensional (3D) locations of the participant's body segments and joints during all research assessment activities. A passive optical motion capture system uses a group of two or more specialized cameras connected to a computer and arranged on a ridged support structure that can emit infrared light via an LED ring and collect infrared light using specialized lenses and their digital image sensors. The infrared light emitted by the cameras is then used to illuminate small spheres called markers that are coated with an infrared reflective substance, which then reflects the emitted infrared light back into the cameras image sensors. This type of optical motion

capture system is called a passive system because the markers themselves are only illuminated by the cameras' LEDs, rather than being able to emit infrared light on their own. Passive motion capture systems can be just as accurate as active motion capture systems, where the markers themselves are LEDs and emit infrared light, and are both more affordable due to their less expensive components and more participant friendly due to their simpler and quicker marker application process that only requires adhesive hook and loop dots and doesn't involve the participant wearing any wires or batteries.

The passive optical motion capture system used for this study included an array of 10 MAC Kestrel 2200 cameras, which are specialized proprietary digital cameras that each have a 2.2MP sensor and an ethernet port that is used for both data connectivity and power, which is facilitated via standard CAT5e ethernet cabling and gigabit network switch hardware and by proprietary power injection hubs and a proprietary Power Over Ethernet (PoE) protocol. Additionally, each camera is equipped with a 1/8" audio port that can be used along with a National Instruments (NI, Austin, TX) Data Acquisition Card (DAQ) for synchronization with other data collection systems and for the collection of external analog and digital signals that are frame synced with the motion capture system data. In addition to the motion capture cameras, the system included one or two Microsoft (Richmond, VA) LifeCam USB webcams which are commercially available webcams that are specifically supported by Motion Analysis for use with their motion capture system to collect synchronized color scene video while the system is recording.

Motion Analysis's Cortex software, version 7.2.6 64-bit, was used to configure and calibrate the motion capture camera system, and was used to record synchronized motion capture, scene video, and analog data during this study. Using Cortex, the motion

capture system was configured to collect motion capture data at a rate of 60Hz, color scene video at a rate of 30Hz, and 12 channels of analog data at a rate of 2520Hz (further analog data details to be discussed in a later section.)

The calibration procedure for the motion capture system is a multistep process that involves two system specific pieces of calibration hardware, a ground plane, and a calibration wand. The ground plane is an L shaped metal assembly that features 4 markers, two built-in bubble levels and three adjustable leveling feet. Marker #1 is located at the point where the two portions of the L frame meet at a ninety-degree angle, while markers #2 and #3 are located on the long arm of the L frame with their centers 200mm and 600mm, respectively from the center of marker #1, and marker #4 is located on the short arm of the L frame with its center 400mm from the center of marker #1. According to the right hand rule, the ground plane is used to define the origin of the 3D volume that will be calibrated for use with the motion capture system, with the long arm of the L frame corresponding to the positive X axis, the short arm corresponding to the positive Y axis, and the positive Z axis corresponding to an imaginary vertical segment centered on marker #1 that is perpendicular to both the long and short arms of the L frame (See image below).

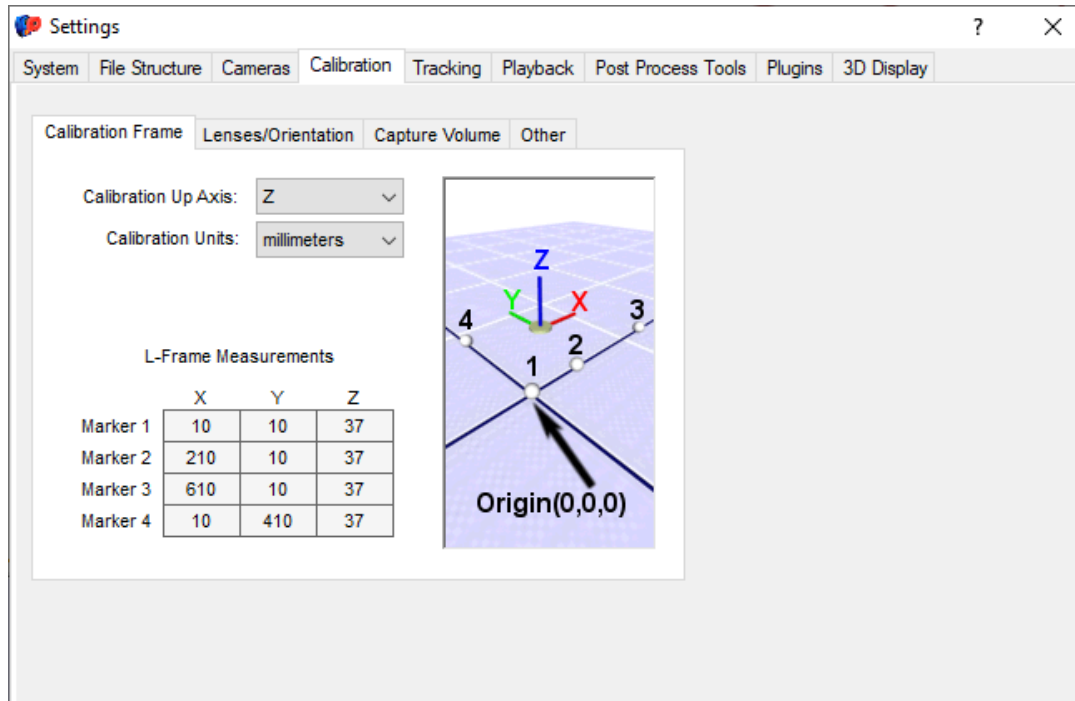


Figure 2.1. Calibration frame configuration in Cortex software.

The calibration wand consists of a telescoping handle with a 500mm rod containing 3 markers fastened at one end with a screw clamp. The rod passed through the center of each of the 3 markers, with the center of marker #1 located at 0mm from one end of the rod, the center of marker #2 located at 380mm from the center of marker #1, and the center of marker #3 located 500mm from the center of marker #1, which is the opposite end of the rod. To begin calibrating the motion capture system, the L frame should be placed in a location such that all 4 of its markers are visible to preferably all, or at least most, of the motion capture cameras to be used for the current motion capture session. In the event that the L frame cannot be placed in the desired location of the origin of the capture volume, an offset can be added to the L frame's setup to enable the origin to be shifted to the desired location once the system is calibrated. Using the Cortex software, the approximate orientation of each motion capture camera needs to be entered based on

the perspective of someone who would be standing in front of each camera, with the available options being upright, upside down, leaning right or leaning left. Once the camera orientation has been entered, the system operator then needs to check the 2D view of each camera to ensure that each camera is only detecting the 4 markers belonging to the L frame and no other markers or infrared reflections. Unwanted reflections are ideally resolved by relocating or covering the offending object or surface, adjusting the brightness of the cameras infrared LEDs, adjusting the cameras threshold setting, adjusting the software's marker filtration settings (maximum size, minimum size, minimum circularity), or by creating an exclusion zone in a given cameras 2D view, called a mask, that instructs the system to ignore any infrared light detected in that portion of its image sensor. Once all unwanted reflections have been addressed, Cortex's built-in calibration procedure can be initiated, and during the first step of this process, the system will collect a single frame of data from each camera containing the location of the L frame markers within that cameras field of view which will be used as the seed frame for the system's calibration algorithm to calculate the approximate 3D locations of all of the cameras relative to the L frame in space, and based on the L frames orientation relative to the surrounding environment, the 3D locations of the origin of the motion capture volume and the orientation of its ground plane. Once this step has been completed, the operator then removes the L frame from the view of all of the cameras, and then brings out the calibration wand to begin the wanding process, which has a similar restriction to the L frame step in that the system will only record camera frames where only the 3 markers of the wand are visible. The wanding process itself consists of waving the wand in a variety of orientations all throughout the intended motion capture

volume to ensure that the system collects sufficient data to accurately detect and compensate for lens distortion and refine its initial estimates of the camera's positions relative to each other and the origin of the volume. Once the operator stops the wandering data collection step, the system then proceeds to perform its calibration calculations using the collected frames of data, and when the calculations are completed, the software then informs the user of the level of accuracy that the system was calibrated to, and if it is sufficient for the current intended subject and volume, the system is ready for use, and if not, the calibration process needs to be repeated until a sufficient level of accuracy is achieved.

To collect motion capture data from the participants in this study, the balance lab's version of the Kessler Foundation's modified Helen Hayes markerset was used when placing markers. The markerset consists of 48 markers whose placement locations correspond to anatomically relevant landmarks such as joint centers and body segments that have been selected in order to enable the data produced by the motion capture system to accurately characterize the 3D spatial movements of the participants joints and body parts while performing research activities (see image below for marker order and locations.).

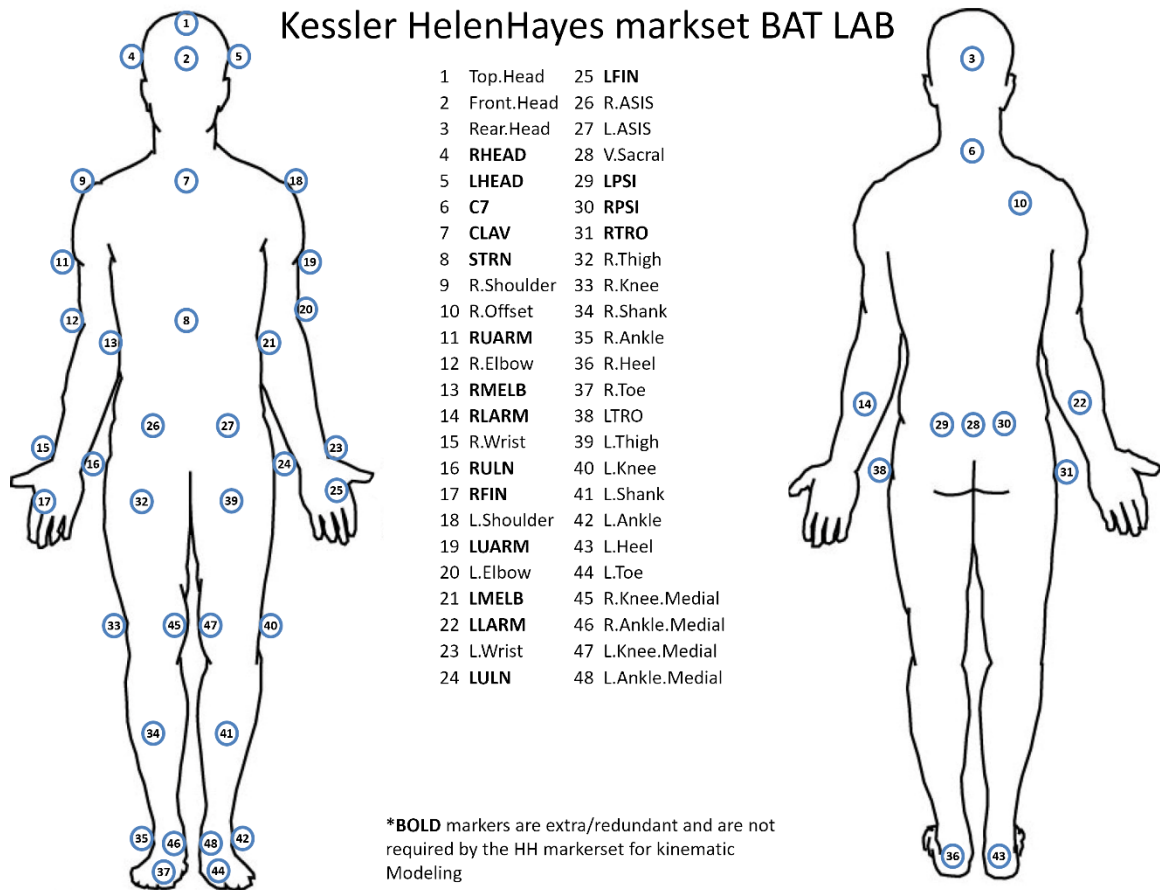


Figure 2.2. Kessler Helen Hayes markerset for balance lab used for kinematic data collection.

Self-adhesive loop dots were placed at the location of each marker, and self-adhesive hook dots were placed on the bottom of the marker posts to facilitate attachment to the participant. 14mm retroreflective markers were used for this study, and various steps were taken to increase the likelihood that markers would remain attached at their intended location for the duration of a given session, including shaving interfering body hair to increase skin adhesion, placing 3M (Maplewood, MN) Blenderm on clothing to improve adhesion when needed or using Blenderm and self-adhesive wrap to hold excess clothing and other material out of the way to avoid occluding or displacing markers during movement. To increase accuracy and reduce the interference of clothing to begin

with, the participants were instructed to wear a short sleeve t-shirt and loose-fitting shorts to enable the maximum number of markers to be placed directly on their skin rather than on their clothing.

Once all markers were placed and checked to be clear of any interference, the markerset templating process within Cortex could be performed. The purpose of the templating process within Cortex is to train the motion capture software to automatically identify and label all of the markers within the markerset in real-time while collecting motion data. This is important for reducing the amount of post processing that needs to be performed on the motion capture data before it can be used for analysis, and it makes it easier to notice if critical markers are being poorly detected or lost during a session to prevent data loss. In order to train the motion capture software, several motion capture trials were recorded and then immediately post processed to provide the necessary. These trials included a static trial where the participant was instructed to stand upright with their arms held straight in front of them and their palms facing inward (Need to include screenshots/Images) such that all markers were able to be detected by the camera, and multiple dynamic trials where the participant was asked to move through the full range of motion that they were expected to use during that motion capture session, included a repeat of the static pose for reference, then leaning forwards and backwards, tilting the head forwards and backwards, leaning left and right, and then turning their head to their left and then to their right (Should likely add images of at least some of these movements/poses as well). Once the static and all dynamic trials were post processed, the performance of the template was tested to ensure accurate auto-identification of all of the markerset markers was being performed in real-time by the software, and any templating

related issues were addressed and resolved before proceeding to collect any additional motion capture data.

Wireless EMG System

A Noraxon (Noraxon USA Inc., Scottsdale, AZ) wireless Electromyography (EMG) system was used to record EMG signals from the participants' lower limbs during all research activities. An EMG system consists of multiple electrodes that are connected to an amplification and control unit, and each electrode consists of three contacts, two are placed adjacent to each other along a line that corresponds to the long axis of the muscle who's electrical activity is to be recorded, and the third contact is placed at a different location to electrically tie the electrode to the participant's skin and reduce unwanted electrical activity on the skin from introducing noise into the signal. In a wired EMG system, the electrodes are directly connected to the amplification and control unit, which is then connected either directly to a computer or to an analog to digital acquisition device, such as an NI DAQ, whereas in a wireless system, the connection between the electrodes and the control unit is facilitated via a wireless data link so that the participant is not tied down to the electrode wiring. In order to facilitate the wireless connection between the electrode and the control unit, the electrode is connected via short wires to a small battery powered module worn by the participant that contains a circuit board and radio transmitter. These components detect the muscle's electrical activity and digitize it, and may also perform some amplification and or filtering, and then transmit the resulting signal back to the control unit which is then directly connected to a computer for digital data capture or connected to a data acquisition card for analog data capture.

EMG signals were recorded bilaterally from the tibialis anterior (TA), soleus (SOL), gastrocnemius (GAST), biceps femoris (BF), vastus lateralis (VAST), and rectus femoris (RF). These muscle were selected as they are predominantly involved in causing flexion and extension about the ankle, knee, and hip, and these joints are essential for maintaining postural stability during standing and perturbed standing by contracting in particular configuration at particular times in what are called muscle synergies [24]–[26]. These muscle synergies are coordinated and configured based on the direction and amplitude of a given perturbation and enable the body to effectively maintain its center of mass (COM) over its base of support [24]–[26]. Additional muscles are known to be involved in synergies for responding to postural perturbations [24]–[26], however several of these muscles are located above the waist and were therefore excluded for the purpose of this study due to the expected signal artifacts that would likely result from the use of the Neurocom’s safety harness, while others are deeper muscles that are more difficult to isolate.

Prior to the application of an electrode to a given location, the application area is prepared by trimming hair if necessary, removing dead skin with a scouring pad, and then cleaning the area with an alcohol wipe to minimize the presence of contaminants that could negatively affect signal quality. To improve the electrical conductivity between the electrode’s contacts and the skin, a conductive gel is placed at the interface between the electrode’s contacts and the skin surface. This is accomplished via the use of self-adhesive dual electrode stickers that are pre-gelled to provide improved signal quality and maintain consistent spacing between the electrode’s two contacts.

After all electrodes and transmitters are properly placed on the participant, the electrodes and transmitters are further secured to the participant via self-adhesive bandages. These bandages are applied using two or more layers to firmly hold the electrodes and transmitters in place while the participant moves, sweats, or accidentally bumps the EMG hardware components on their person during study activities. While the adhesives on the electrodes and transmitters are generally sufficient to hold them in place, they can fail due to excess sweating and are particularly weak to shearing forces, while the use of the self-adhesive wraps virtually eliminates the need to re-apply EMG components after the initial setup. To ensure participant comfort and avoid causing any skin indentations, the participant is asked to confirm that none of the wraps are too tight or otherwise affecting their ability to move, and any issues are resolved prior to proceeding with study activities.

MVC Collection

EMG data collected from the same muscle during the same activity with the same individual can vary greatly from session to session and day to day due to changes in the electrical conditions of the collection site, which may result from slight variations in the skin preparation procedure performed or minor differences in electrode placement between sessions [27], [28]. As a result of this variability, quantitative comparisons of EMG within or between subjects require the data to be normalized in some way, and a commonly used method is to use each muscle's maximum voluntary contraction (MVC) as a reference value, such that subsequent muscle activity can be expressed as a percentage of the MVC [27], [28]. An MVC is performed by having the subject perform

an isometric contraction across a single joint against static resistance, such as straps or the braced limb of a trained member of the research team, such that the subject's limb does not move during the contraction [27], [28]. As the name implies, an MVC should ideally represent the absolute maximum muscle output that can be generated by the muscle in question [28], however depending on the subject population and the type of movements being recorded, ascertaining the actual maximum muscle output may not be practical or even possible [27], [28], so alternative approaches need to be used [27].

For this study, MVC were performed first on the left limb for each muscle to be tested, and then on the right limb, with the participant on a height adjustable exam table, and resistance was provided by a trained member of the study team. For each fifteen second trial, the participant was instructed to relax for the first and last five seconds of the trial, and to push against the applied resistance as much as possible for the middle five seconds. The MVC for the TA was performed with the participant positioned on their back with their leg straight, and they were asked to move their foot towards their upper body. With the participant still on their back, they were then asked to bend their knee and place their foot flat on the surface of the exam table while pushing their heel into the surface of the table for the SOL MVC. While remaining on their back once again, the participant was asked to straighten their leg and move their foot away from their upper body, as if they were pressing on a gas pedal, to record the MVC for the GAST. To perform the MVC for the RF, the participant was asked to carefully flip onto their stomach, to avoid displacing any of the EMG electrodes or transmitters, after which the member of the study team lifted their lower leg into a vertical position to provide resistance as the participant was instructed to move their foot towards their backside. The

MVCs for the VAST and the RF were performed at the same time with the participant in a seated position and their legs hanging freely off the side of the exam table. While in this position, the member of the study team braced themselves in a chair in front of the participant and instructed them to kick outward as they resisted the movement. All MVC trials were monitored for performance and signal quality during collection, and any problematic trials were repeated as necessary.

Instrumented Balance Platform

The Neurocom Smart Equitest Clinical Research System (CRS) (Natus Medical Inc. Pleasanton, CA) was used to provide precise, preprogrammed perturbations to the participants' base of support in the anterior-posterior (AP) direction during both the Standard Trial and Perceived Perturbation Threshold (PPT) balance assessments that will be described in detail below. The CRS consists of an instrumented mobile platform with a separate force plate for each foot, an integrated overhead harness to ensure participant safety during all activities, and is capable of horizontal movement in the AP direction and rotation movement about the participant's ankles. The two separate force plates enable the CRS to monitor the participant's combined COP in the horizontal plane, as well as the COP for each foot individually. The Neurocom platform collects COP, platform position, and other measures at a rate of 100Hz.

Intersystem Connectivity and Synchronization

In addition to enabling EMG data to be streamed into Cortex, the NI DAQ was also used to synchronize data collection between Cortex and the Neurocom platform by sending a sync pulse to the platform's synchronization module.

2.4 Data Collection Procedures for Research Assessments

Quiet Standing

After the completion of preparations for the platform trials, a sixty second quiet standing trial was performed. During this trial, all data streams were collected, but no perturbation was delivered, with the participant being instructed to stand up straight and look straight ahead for one minute.

Standard Trials Balance Assessment

After the completion of the quiet standing trial, sinusoidal perturbations were delivered in three groups of five trials each. Each group of perturbations was delivered at an increasing frequency, 0.33Hz, 0.5Hz, and then 1Hz, with the perturbation amplitudes decreasing from 10 mm down to 2 mm for each set of five trials.

Each standard trial was divided into three equal parts, a period of quiet standing, followed by a period sinusoidal perturbation, and finally a second period of quiet standing. In order to provide perturbation profiles with complete cycles at each frequency, perturbation trials for 0.5 Hz and 1 Hz were 15 seconds in duration, while 0.33 Hz perturbation trials were 18 seconds long. During these trials, the participant was instructed to stand up

straight, look straight ahead, and maintain their balance for the duration of the trial. No verbal response was needed from the participant during this stage of testing.

These standard trials were performed to enable comparisons to be made between individuals and groups over a consistent set of perturbations at high enough amplitudes that they would be perceivable by all participants.

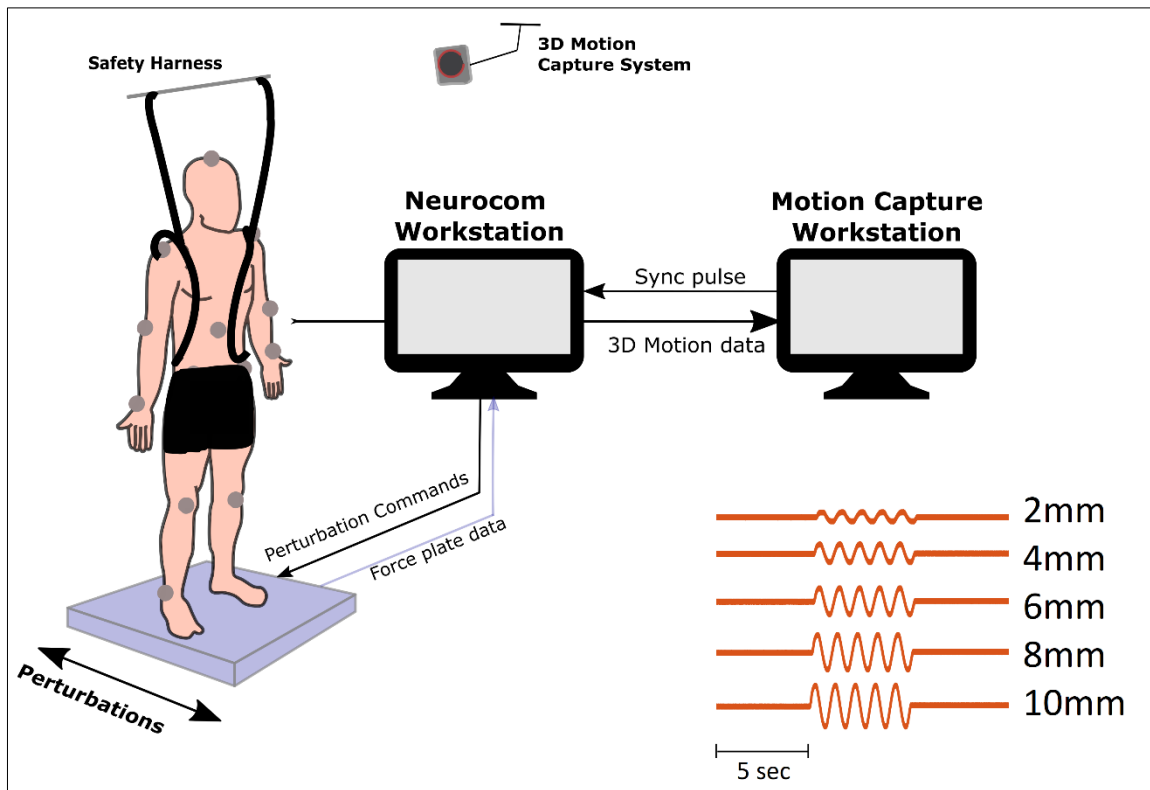


Figure 2.3. Experimental setup for Standard Trials Assessment [29].

Perceived Perturbation Threshold Balance Assessment

To determine the participant's perception threshold for perturbations at a given frequency, participants were instructed to stand up straight on the platform, look straight ahead, maintain their balance, and at to report if they had felt any movement during each trial. Each frequency set consisted of 21 trials, with the first trial of each frequency

beginning with the 4mm perturbation trial. A Single Interval Adjustment Matrix (SIAM) algorithm [22] was used to adjust the amplitude of each subsequent trial in a staircase manner based on the participant's response of yes or no to the question of whether they had felt the platform move, with a Hit being the correct identification of movement, a Miss being a failure to identify movement, a Correct Rejection being the correct identification of a non-movement trial, and a False Alarm being the incorrect identification of the non-movement trial as a movement trial. The PPT assessment was performed at 0.33Hz, 0.5Hz, and at 1 Hz, with the trial durations set according to frequency as mentioned above for the standard trials (15 second trial duration for 0.5 and 1 Hz, and 18 seconds for 0.33Hz). The first and last third of each trial consisted of quiet standing, and the middle third consisted of platform movement, or no platform movement, depending on the above-mentioned algorithm.

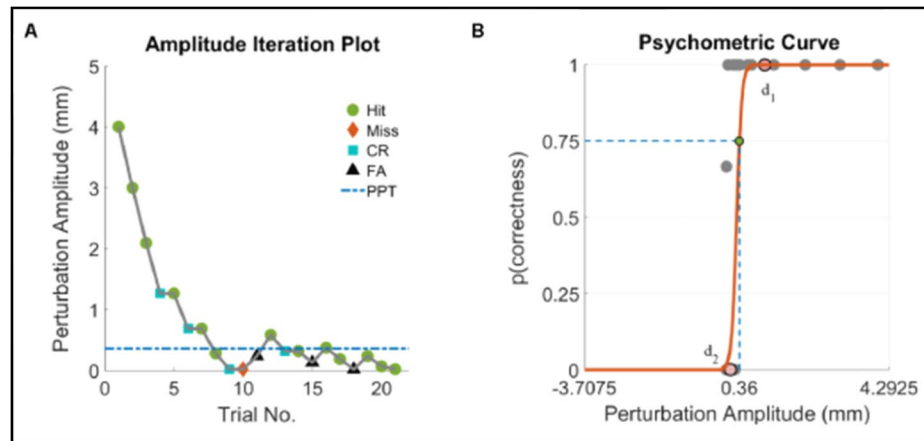


Figure 2.4. A) Progression of perturbation amplitudes during a single frequency of the PPT featuring correct responses until the amplitude drops below the participant's PPT assessment based on the SIAM algorithm. B) Example of the psychometric curve used to identify each participant's PPT. [22]

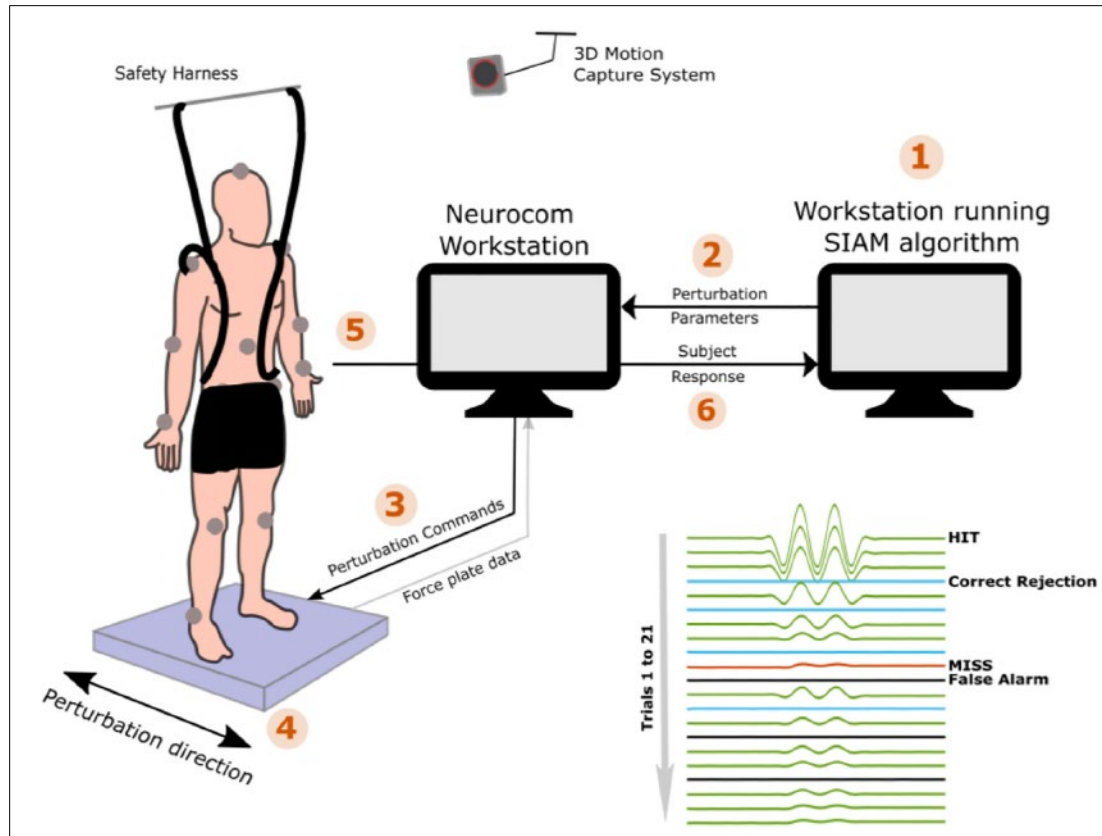


Figure 2.5. Simplified experimental setup for Perceived Perturbation Threshold Balance Assessment as described above, showing the interconnections of the equipment and flow of information out of and back into the SIAM algorithm for every subsequent perturbation. [22]

2.5 Clinical Assessments

After being screened and consented into the study, all participants underwent the following clinical assessments of static and dynamic balance to gauge their post TBI impairment and fall risk: Berg Balance Scale (BBS), 5 Meter Walk Test (5MWT), 10 Meter Walk Test (10MWT), Timed Up and Go (TUG). The BBS consists of 14 tasks that include sitting, standing, transferring, lifting, and reaching, with each task being scored on a 0-to-4-point scale. A score of 4 represents the ability to properly perform the task without any assistance, while a score of 0 represents the inability to perform the task. The 5MWT and the 10MWT consist of a straight, flat, unobstructed walking course that is 5

or 10 meters long, respectively. In both measures, the participant was asked to walk as quickly but as safely as possible from the start to the end of the course, and then to return to the start of the course with the same instructions after a brief pause, with their performance recorded as the average of the two walks. The TUG asks the participant to stand from a sitting position, walk 3 meters to a cone, walk around the cone in either direction, and then walk 3 meters back to their chair and return to sitting position while the task is being timed. The BBS and TUG measure the participant's static balance abilities, ability to transition between static tasks, and their ability to transition from static to dynamic tasks, while the walking tests measure the participant's dynamic balance during an extended locomotor task. These clinical assessments were performed for all participants in all groups, and participant safety was provided by a spotter during all clinical assessments.

2.6 Data Processing

Motion capture trials were labeled, and gap filled in Cortex after data collection, and once all of the trials for a single session were cleaned, the subject's height and weight were entered into the software so that the skeletal model could be updated to match the subject and kinematic and COM measures could be calculated. The data was then filtered using Cortex's built in smoothing tool which applied a 6Hz Butterworth filter. A custom Cortex script was then developed and used to batch export that session's data out of Cortex into text files in preparation for the data to be imported into MATLAB for analysis along with data from the Neurocom software using its built-in utilities.

A script was then developed and used to automatically import all data types for a given subject into MATLAB and organize them within a monolithic structured array for each subject which was then saved as individual .mat files to substantially increase processing speeds and simplify analysis by automatically detecting and addressing any trial or variable name issues during the import process to enable robust and consistent access to all subject data. These uniformly organized data structures were then used to rapidly generate and iterate scripts for creating data plots and calculate outcome variables throughout the course of data analysis.

2.7 Statistical Analysis

Scatter plots were generated comparing the range of motion of the hip and ankle joints for all perturbation frequencies and amplitude with the clinical assessments and the PPT, and correlations were then run on each of these comparisons in MATLAB, with linear regressions and ANOVAs run on all correlations with an absolute R value greater than 3.0. SPSS version 26 was used to calculate repeated measures ANOVAs for all kinematic outcomes, and independent sample t-tests were performed on any outcomes with significant between-subjects effects, with significance for the t-tests at $p < 0.01$ after Bonferroni corrections.

CHAPTER 3

EVALUATING SENSORY ACUITY AFTER A TBI

3.1 Methods and Results

In order to objectively measure sensory acuity as it pertains to a person's ability to perceive perturbations to their base of support during standing post TBI, and to ascertain whether or not a relationship exists between sensory acuity post TBI and functional measures of static and dynamic balance, the Perception of Perturbation Threshold (PPT) assessment was developed. The PPT and clinical balance assessments were then performed with a group of 10 individuals post TBI and 11 aged matched healthy controls, and the results were published in the August 2020 issue of *Frontiers in Neuroscience*, volume 14 [30]. Study procedures were performed as outlined above in chapter 2, including the berg balance scale, timed up and go, 5-meter walk test, and 10-meter walk, which were then followed by the PPT assessment.

The scores for all function assessments were significantly lower for the TBI group compared to the HC group. For the BBS, the mean score for the TBI group was 48.8 ± 6.43 compared to the HC group's score of 55.91 ± 0.3 ($p = 0.007$). On the 5MWT, the TBI group's mean time was 4.61 ± 1.18 seconds compared to the HC group's time of 2.96 ± 0.58 seconds ($p = 0.001$), and on the 10MWT, the TBI groups average time was 9.34 ± 2.6 seconds compared to the HC group's mean time of 5.47 ± 0.91 seconds ($p < 0.005$). For the TUG, the mean time for the TBI group was 12.7 ± 3.6 seconds compared to the mean time for the HC group which was 7.41 ± 1.38 seconds ($p < 0.005$).

The PPT assessment yielded the highest variability in perception thresholds for the 0.33Hz perturbations for both groups, while the 1Hz perturbations showed the lowest

variability for both groups. A mixed-design analysis of variance (ANOVA) demonstrated significant main effects of condition [$F(1, 19) = 44.35, p < 0.005$] and perturbation frequency [$F(2, 38) = 42.14, p < 0.005$] on the PPT, as well as interactions between condition and perturbation frequency ($F(2, 38) = 9.65, p < 0.005$). Post-hoc analysis showed a significant difference in the PPT values between the TBI and HC groups for all three perturbation frequencies ($p < 0.006$), with mean PPT values for TBI group of 2.97 ± 1.0 , 2.39 ± 0.7 , and 1.22 ± 0.4 , and mean PPT values for HC group of 1.03 ± 0.6 , 0.89 ± 0.4 , and 0.42 ± 0.2 for the 0.33Hz, 0.5Hz, and 1Hz perturbations, respectively. Within-group post hoc analysis demonstrated no significant difference between 0.33Hz and 0.5Hz perturbation frequencies for both groups (TBI $p = 0.047$, HC $p = 0.298$), but significant differences in the PPT were observed between 1Hz and 0.5Hz perturbations (TBI $p < 0.006$, HC $p = 0.002$) and 1Hz and 0.33Hz perturbations (TBI $p < 0.006$, HC $p = 0.003$) for both groups.

A significant positive correlation was found between the PPT at 1Hz and completion time for the TUG ($p = 0.008$), the 5MWT ($p = 0.034$), and the 10MWT ($p = 0.012$) for individuals post TBI, but no significant correlation was found between the PPT at 0.5Hz and completion time (TUG $p = 0.29$, 5MWT $p = 0.34$, 10MWT $p = 0.13$), or between the PPT at 0.33Hz and completion time (TUG $p = 0.14$, 5MWT $p = 0.28$, 10MWT $p = 0.18$) post TBI. No significant correlation was found between the PPT at any frequency and completion time for the TUG, 5MWT, or 10MWT for the HC group. Somewhat similarly, a significant negative correlation was observed between the PPT at 1Hz and the BBS for the TBI group ($p = 0.037$), while no significant correlations were found for the PPT at 0.33Hz ($p = 0.09$) or at 0.5Hz ($p = 0.17$) post TBI, or between the

PPT at any frequency and the BBS for the HC group. In light of the significant correlations that were found for the TBI group between the PPT at 1Hz and all four clinical balance measures, a subsequent investigation was initiated in an attempt to ascertain the presence of any detectable lower limb biomechanical differences that might indicate shifts in the postural control strategies used by the participants during the perturbations that might also correlate with the above-mentioned clinical balance measures.

CHAPTER 4
KINEMATIC ANALYSIS OF PERTURBED STANDING AFTER A TBI: A
PILOT STUDY

4.1 Methods and Results

A preliminary analysis was performed on a subset of data from four individuals with chronic TBI and four aged match healthy controls early on in the study, and was published as a four-page paper for the IEEE's 2021 Engineering in Medicine and Biology Conference (EMBC) [29]. Study procedures were performed as outlined above in chapter 2, including the berg balance scale, timed up and go, 5-meter walk test, and 10-meter walk, and the Standard Trials Balance Assessment. In addition to the clinical assessment scores, peak to peak range and root mean square (RMS) values were calculated for the hip, knee, and ankle joints during the 5-second perturbation period for all amplitudes using MATLAB (Mathworks Inc., Natick, MA), and statistical analysis of the data was performed with SPSS version 26 (IBM Corp., Armonk, NY).

Demographics and functional assessments are shown in the table below (Table 3.1), with the TBI groups mean scores being 49.25 for the BBS, 4.21s for the TUG, 8.01s for the 5MWT, and 12.40 seconds for the 10MWT, while the HC groups mean scores were 56, 3.02 seconds, 5.76 seconds, and 7.42 seconds, respectively for the same measures. The difference between the two groups' functional assessment scores indicates the presence of clinically relevant static and dynamic balance impairments in the TBI group compared to the HC group, with the TBI group's scores being lower and slower than the HC group's scores.

The mean range and RMS of movement about the lower limb joints are shown in Figure 3.1 for both the HC and TBI groups across all conditions. The HC group's mean range about the ankle in the sagittal plane for the 10, 8, 6, 4, and 2mm perturbations were, $4.17 \pm 0.81^\circ$, $5.02 \pm 1.46^\circ$, $2.65 \pm 0.83^\circ$, $2.80 \pm 0.78^\circ$, and $1.85 \pm 1.21^\circ$, respectively. The TBI group's mean range about the ankle were $5.17 \pm 1.91^\circ$, $2.94 \pm 2.05^\circ$, $1.95 \pm 0.26^\circ$, $1.86 \pm 0.87^\circ$, and $1.48 \pm 0.31^\circ$, respectively. The TBI group showed a higher mean range than the HC group for the 10mm perturbation, but their mean range was smaller than the HCs for the other 4 conditions, and this pattern was also reflected in the RMS values (Figure 3.1).

The mean range of the HC group's knee angle in the sagittal plane for the 10, 8, 6, 4, and 2mm perturbations were $5.13 \pm 2.50^\circ$, $6.67 \pm 5.09^\circ$, $2.72 \pm 0.99^\circ$, $2.30 \pm 1.16^\circ$, and $1.44 \pm 0.51^\circ$, respectively, and the mean range for the TBI group's knee angle in the sagittal plane for the same perturbations were $9.97 \pm 5.70^\circ$, $4.85 \pm 5.08^\circ$, $1.85 \pm 0.60^\circ$, $2.12 \pm 1.08^\circ$, and $1.48 \pm 0.59^\circ$, respectively. The TBI group's range was larger than the HC group's for the 10 and 2mm perturbations, and decreased in line with the decreasing perturbation amplitudes, with the exception of the 4mm perturbation that increased. The HC group's range increased for the 8mm trial, but then decreased in line with the decreasing perturbation amplitudes for the remaining trials. These patterns were mostly reflected in the mean RMS values as well, except both group's values increased for the 4mm condition, and the TBI group's mean RMS was smaller than the HC group's for all conditions except the 10mm perturbation, as shown in Figure 3.1.

The HC group's mean range about the hip in the sagittal plane for the 10, 8, 6, 4, and 2mm perturbations were $3.50 \pm 1.44^\circ$, $3.32 \pm 1.56^\circ$, $2.22 \pm 1.30^\circ$, $2.08 \pm 0.96^\circ$, and

1.31 ± 0.62°, respectively. The TBI group's mean range about the hip for the same perturbations were 12.97 ± 11.86°, 5.98 ± 3.14°, 3.77 ± 2.53°, 3.73 ± 1.95°, and 2.01 ± 0.50°, respectively. The TBI group's mean range values were larger than the HC group's for all conditions, and both the TBI and HC group values decreased with perturbation amplitude for all conditions. The mean RMS values for the TBI group were larger than the HC group's for all conditions and decreased with perturbation amplitude for all conditions, while the HC group's mean instead increased slightly for the 8 and 4mm conditions.

No significant outliers were detected in the data during analysis, and the joint range of movement was found to be normal ($p > 0.05$) for 12 out of the 15 mean range values of joint movement (dependent variable). Mauchly's test of sphericity for the platform perturbations was non-significant ($p > 0.05$) but was significant for the joints ($p = 0.002$). As a result, sphericity was assumed for the within-subject factor, platform perturbations, while sphericity was not assumed for the within-subject factor, joints, and the metrics from Greenhouse-Geisser are reported. The main effect of joints was not significant [$F(1.5,9) = 1.615, p = 0.247$], however, a significant joint*group interaction effect was observed [$F(1.5,9) = 4.731, p = 0.047$], and this interaction effect shows that mean range values of joint movement had different effects for the TBI and HC groups. The main effect of platform perturbation was significant [$F(4,24) = 9.434, p < 0.001$], which showed that the platform perturbations were different, however the platform perturbation*group interaction effect was not significant [$F(4,24) = 2.731, p = 0.053$], tests of between-subjects effects showed that the TBI and HC groups were not significantly different [$F(1,6) = 0.719, p = 0.429$].

Prior literature has demonstrated that balance dysfunction after a TBI can include muscle weakness, reduced coordination and motor control, and a decreased ability to detect the position and configuration of one’s body in space and changes to their base of support [30]–[32]. As such, it was hypothesized that the TBI group would have a larger range of motion about their ankles, or motion about both their hip and ankle joints. Consequently, the fact that the preliminary data showed the TBI group’s larger range and RMS about the hip joint, the HC group’s larger range and RMS about the ankle joint, and the fact that the joint*group interaction affect was significant, were in line with expectations, and helped inform the decision to expand the current analysis to include additional subjects and perturbation amplitudes.

Table 4.1. Demographics and Functional Assessments.

Group	ID	Level of Injury	Age	Height (cm)	Weight (kg)	TSI (yrs.)	BBS	TUG (s)	5MWT (s)	10MWT (s)
HC	001	-	53	177.17	68.95	-	56	2.77	5.62	7.28
HC	002	-	40	173.99	67.36	-	56	2.39	4.74	7.87
HC	003	-	45	170.18	116.57	-	56	3.27	6.08	7.63
HC	004	-	48	154.94	86.18	-	56	3.64	6.61	6.88
HC		Mean	46.50	169.07	84.77		56	3.02	5.76	7.42
		SD	5.45	9.84	22.85		0.00	0.55	0.79	0.43
TBI	001	Mild	49	172.72	66.68	1.67	46	4.77	9.63	16.10
TBI	002	Moderate/Severe	54	156.21	73.48	2.70	52	4.32	8.16	10.12
TBI	003	Mild	56	166.37	119.29	10.34	55	4.25	8.24	11.84
TBI	004	Moderate/Severe	35	182.88	69.40	9.38	44	3.50	6.02	11.54
TBI		Mean	48.50	169.55	82.21	6.02	49.25	4.21	8.01	12.40
		SD	9.47	11.19	24.88	4.47	5.12	0.52	1.49	2.58

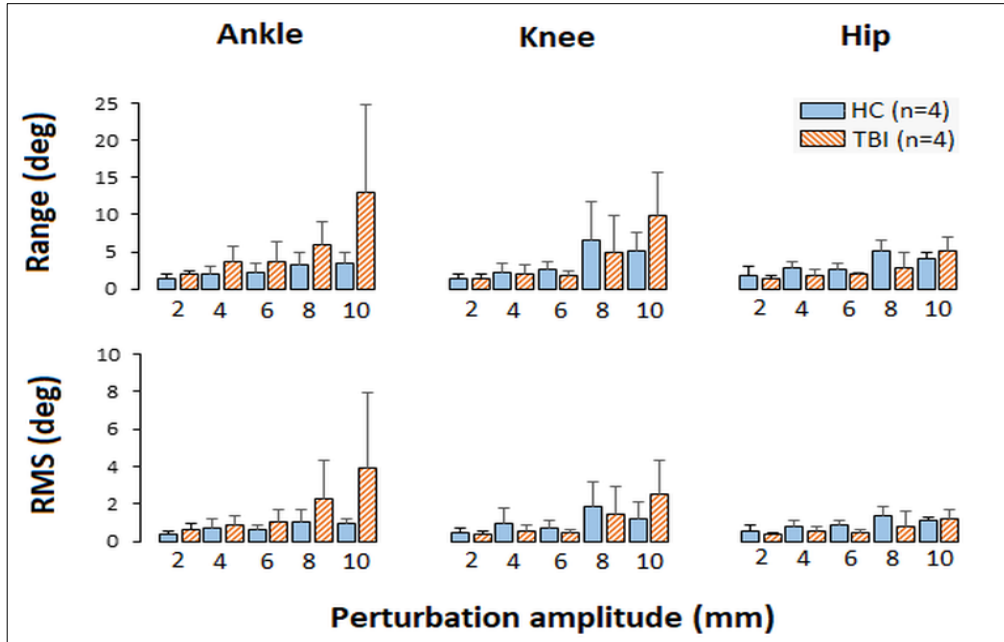


Figure 4.1. The mean range and RMS values for hip, knee, and ankle joints across all perturbation amplitudes for the HC (n=4) and TBI (n=4) groups. The perturbation amplitudes are sorted from low to high order for intuitive presentation of the data.

CHAPTER 5

RESULTS

5.1 Functional Assessments

Twelve adults between the ages of 24 and 60 (mean 49.92 ± 12.43 years) who had previously experienced a TBI with a mean time since injury of 9.98 ± 15.33 years were recruited for participation in the study. Nine healthy individuals between the ages of 40 and 64 (mean 52.11 ± 7.75 years) were recruited for participation to serve as healthy control (HC) group for comparison. The scores for all function assessments were significantly lower for the TBI group compared to the HC group. For the BBS, the mean score for the TBI group was 48.42 ± 7.75 compared to the HC group's score of 55.78 ± 0.44 , and the TUG mean time for the TBI group was 15.86 ± 14.70 seconds compared to the mean time for the HC group which was 7.11 ± 1.03 seconds. On the 5MWT, the TBI group's mean time was 6.42 ± 7.19 seconds compared to the HC group's time of 3.00 ± 0.63 seconds, and on the 10MWT, the TBI group's average time was 12.25 ± 12.62 seconds compared to the HC group's mean time of 5.54 ± 0.99 seconds (Table 5.1).

Table 5.1. Participant Demographics and Functional Assessments

Group	#	Level of Injury	Age	Height (cm)	Weight (kg)	TSI (yrs)	BBS	TUG (s)	5MWT (s)	10MWT (s)
HC	001		40	173.99	67.36		56	7.87	2.39	4.74
HC	002		48	154.94	86.18		56	6.88	3.64	6.61
HC	003		54	160.02	83.91		55	6.62	2.96	5.66
HC	004		57	165.10	88.45		55	7.25	3.25	5.86
HC	005		41	158.75	76.20		56	7.81	3.34	6.37
HC	006		55	162.56	77.11		56	6.10	2.70	5.03
HC	007		55	167.64	70.31		56	6.75	2.64	4.86
HC	008		55	178.00	83.91		56	5.65	2.03	3.87
HC	009		64	173.00	72.57		56	9.06	4.05	6.84
HC (n = 9)		Mean	52.11	166.00	78.45		55.78	7.11	3.00	5.54
		SD	7.75	7.77	7.50		0.44	1.03	0.63	0.99
TBI	001	Severe	59	178.44	143.79	6.66	49	12.41	4.15	10.05
TBI	002	Mild	51	180.34	113.85	5.24	54	8.07	3.11	6.30
TBI	003	Severe	52	171.45	96.39	6.77	54	9.78	3.98	7.83
TBI	004	Mild	32	168.91	58.51	3.61	56	7.47	3.10	5.24
TBI	005	Mild	56	166.37	119.29	10.34	55	11.84	4.25	8.24
TBI	006	Moderate	60	154.31	73.48	57.81	34	17.60	6.30	13.08
TBI	007	Severe	60	175.90	88.68	7.48	44	15.18	5.34	9.76
TBI	008	Mild	60	181.61	115.21	1.67	48	16.90	6.69	14.20
TBI	009	Moderate/Severe	54	156.21	73.48	2.70	52	10.12	4.32	8.16
TBI	010	Moderate/Severe	24	170.18	62.60	1.31	35	61.29	28.94	51.39
TBI	011	Mild	56	182.88	86.18	6.82	56	8.16	3.36	6.81
TBI	012	Moderate/Severe	35	182.88	69.40	9.38	44	11.54	3.50	6.02
TBI (n = 12)		Mean	49.92	172.46	91.74	9.98	48.42	15.86	6.42	12.25
		SD	12.43	9.82	26.44	15.33	7.75	14.70	7.19	12.62

5.2 Sensor Acuity Measure

The TBI group's mean PPTs were higher than the HC group's for all perturbation frequencies. For the 0.33Hz perturbations, the mean PPT for the TBI group was 2.66 ± 1.51 mm, which was 1.65 mm higher than the HCs which was 1.01 ± 1.05 mm and was the perturbations frequency with the largest difference in thresholds. The next smallest difference in PPT was 0.70 mm for the 0.5Hz perturbations, where the mean PPT for the TBI group was 1.66 ± 1.21 mm, and the mean for the HC group was 0.96 ± 1.19 mm.

The 1Hz perturbations yielded the smallest difference between the group’s PPTs at 0.42 mm, with the TBI group’s mean being 0.69 ± 0.60 mm and the HC group’s mean being 0.27 ± 0.33 mm (Table 5.2).

Table 5.2. Perceived Perturbation Threshold by Perturbation Frequency

Group	#	0.33Hz			0.55Hz			1Hz		
		PPT Using Reversals	PPT Using Intervals	Average PPT	PPT Using Reversals	PPT Using Intervals	Average PPT	PPT Using Reversals	PPT Using Intervals	Average PPT
HC	001	0.84	0.04	0.44	0.80	0.39	0.59	NA	NA	NA
HC	002	0.77	0.21	0.49	0.05	0.02	0.04	0.04	0.02	0.03
HC	003	1.65	1.80	1.72	1.18	1.18	1.18	0.30	0.19	0.25
HC	004	0.75	0.72	0.74	0.09	0.20	0.15	NA	NA	NA
HC	005	0.23	0.07	0.15	0.74	0.64	0.69	0.21	0.11	0.16
HC	006	0.50	0.44	0.47	0.57	0.49	0.53	0.21	0.14	0.17
HC	007	0.29	0.03	0.16	0.28	0.31	0.30	0.08	0.04	0.06
HC	008	1.84	1.27	1.55	1.26	1.21	1.23	0.28	0.16	0.22
HC	009	3.30	3.43	3.37	3.91	3.98	3.95	0.99	1.01	1.00
HC (n = 9)	Mean	1.13	0.89	1.01	0.99	0.93	0.96	0.30	0.24	0.27
	SD	0.99	1.13	1.05	1.18	1.21	1.19	0.32	0.35	0.33
TBI	001	4.98	4.84	4.91	3.34	3.43	3.38	1.40	1.51	1.46
TBI	002	2.90	3.11	3.01	2.66	2.81	2.73	0.94	0.91	0.92
TBI	003	2.95	3.07	3.01	1.15	1.27	1.21	1.20	1.30	1.25
TBI	004	NA	NA	NA	0.52	0.21	0.36	NA	NA	NA
TBI	005	0.74	0.45	0.60	0.06	0.02	0.04	0.02	0.02	0.02
TBI	006	4.43	4.57	4.50	2.84	3.23	3.04	NA	NA	NA
TBI	007	2.09	2.13	2.11	1.73	1.73	1.73	1.19	0.95	1.07
TBI	008	3.05	3.70	3.37	2.63	2.73	2.68	1.52	1.39	1.45
TBI	009	2.97	3.15	3.06	2.67	2.78	2.73	0.43	0.27	0.35
TBI	010	0.30	0.33	0.31	0.32	0.02	0.17	0.02	0.02	0.02
TBI	011	1.77	1.59	1.68	0.93	1.14	1.03	0.33	0.20	0.26
TBI	012	NA	NA	NA	0.94	0.74	0.84	0.04	0.05	0.05
TBI (n = 12)	Mean	2.62	2.70	2.66	1.65	1.68	1.66	0.71	0.66	0.69
	SD	1.46	1.56	1.51	1.13	1.28	1.21	0.60	0.61	0.60

5.3 Kinematic Measures

Perturbations Delivered at 0.33 Hz

The TBI group’s mean hip range of motion for the 0.33Hz perturbations were higher than the HC group’s mean range for four out of the five perturbations amplitudes. For the

10mm perturbation the mean hip range of motion for the TBI group was 3.28 ± 5.43 degrees compared to the HC group's mean which was 3.21 ± 0.76 degrees, and for the 8mm perturbation, the mean hip range of the TBI group was 2.25 ± 3.07 degrees compared to the HC group's mean which was 1.47 ± 0.67 degrees. The trend between the two groups was then interrupted for the 6mm perturbation where the HC's group's mean was higher at 1.56 ± 1.84 compared to the TBI group's at 1.17 ± 0.86 degrees, but then returned for the remaining 4mm and 2mm perturbations as the TBI group's mean hip range of motion was once again larger than the HC group's, with the TBI group's means being 1.43 ± 1.14 degrees and 1.95 ± 3.62 degrees, respectively compared to the HC group's mean of 1.15 ± 0.58 degrees and 1.07 ± 0.91 degrees, respectively (Figure 3.1). Sphericity was not assumed for the hip range of motion at 0.33Hz ($p < 0.001$) and there were no significant within-subject effects for amplitude or amplitude*group with the Greenhouse-Geisser adjustment [$F(1.935,36.760) = 2.432, p = 0.103$ and $F(1.935,36.760) = 0.254, p = 0.770$, respectively] or significant between-subject effects [$F(1.000,19.000) = 0.236, p = 0.633$].

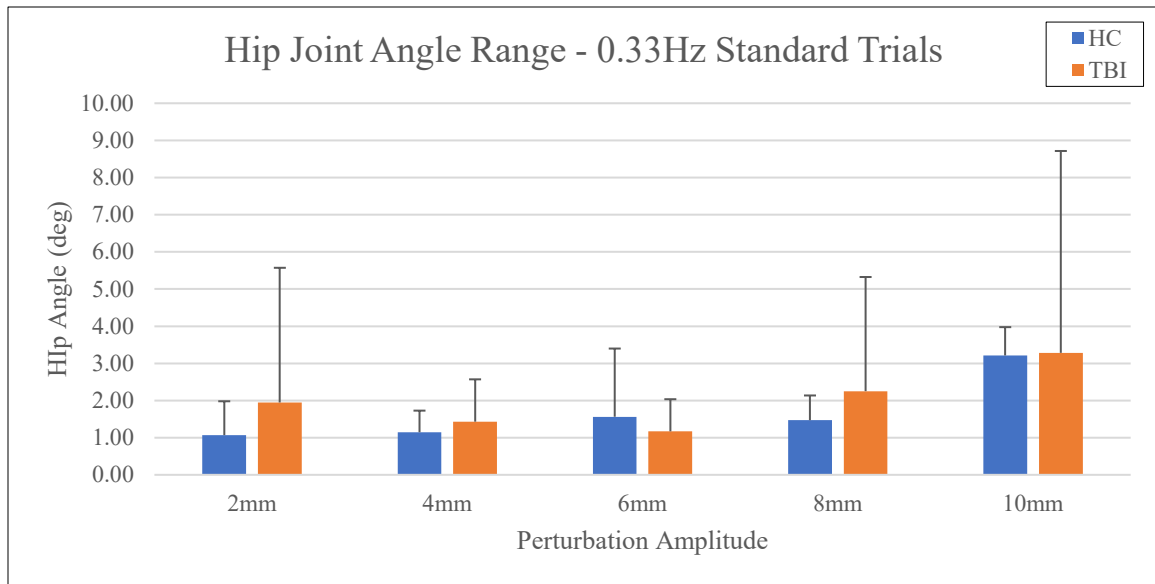


Figure 5.1. Mean hip joint values for HC and TBI during perturbations delivered at 0.33Hz.

The mean knee range of motion for the TBI group was also larger than the HC group's mean for four out of the five perturbation, but did not match the pattern seen for the hip joint as the TBI group's mean range of motion for the 10mm perturbation was smaller at 2.13 ± 2.02 degrees compared to the HC group's mean of 4.82 ± 2.32 degrees. TBI group's mean range of motion was larger than the HC group's for the remaining perturbation coming in at 2.40 ± 2.49 degrees vs. 1.96 ± 1.55 degrees, 1.83 ± 2.60 degrees vs. 1.17 ± 0.45 degrees, 0.98 ± 0.67 degrees vs. 0.85 ± 0.29 degrees, and 0.90 ± 0.86 degrees vs. 0.72 ± 0.35 degrees for the 8, 6, 4, and 2mm perturbations, respectively (Figure 3.2). Like hip, sphericity was not assumed for the knee range of motion at 0.33Hz, but after Greenhouse-Geisser adjustments significant within-subject effects were found for both amplitude [$F(2.005,38.100) = 10.889, p < 0.001$] and amplitude*group [$F(2.005,38.100) = 4.324, p = 0.020$] though no significant between-subject effect was found [$F(1.000,19.000) = 0.346, p = 0.563$].

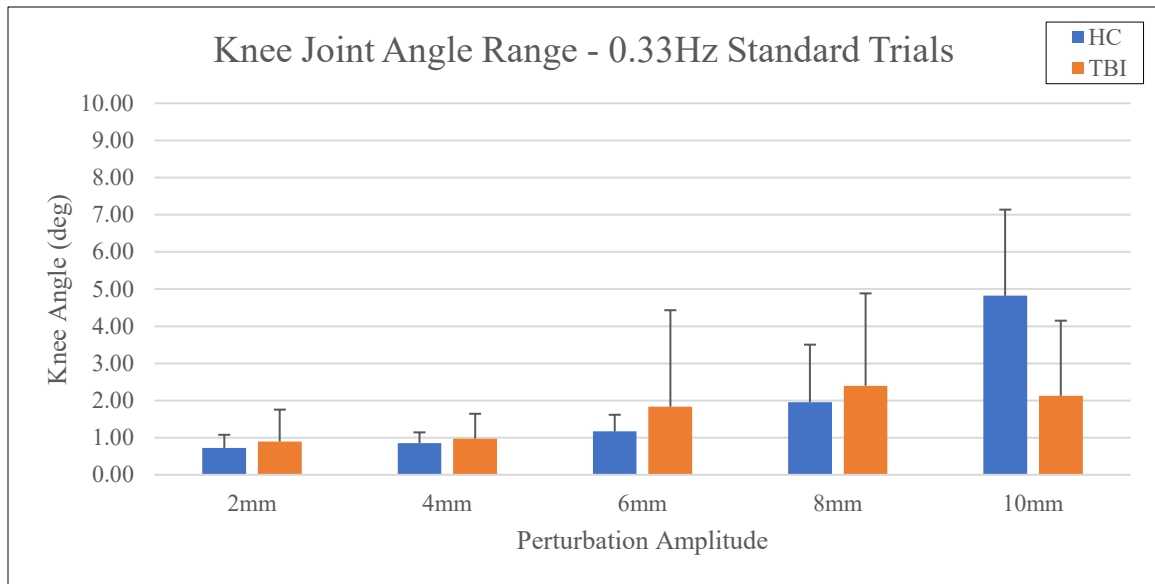


Figure 5.2. Mean knee joint values for HC and TBI during perturbations delivered at 0.33Hz.

About the ankle, the mean range of motion for the split between the two groups with the TBI group’s mean being higher for two perturbations and the HC group’s mean being higher for another two perturbations, and the two groups means being essentially the same for the final perturbation amplitude. For the 10 and 8mm perturbations, the HC group’s mean ankle ranges of motion were larger at 3.12 ± 0.98 degrees and 1.83 ± 1.06 degrees, respectively compared to the TBI group’s 2.90 ± 4.83 degrees and 1.73 ± 1.21 degrees, respectively. Both groups’ mean ranges of motion were very similar for the 6mm perturbation with the TBI group’s mean coming in at 1.38 ± 1.28 degrees compared to the HC group’s mean of 1.37 ± 0.65 degrees. The 4 and 2mm perturbations resulted in larger mean ranges of motion about the ankle for the TBI group of 1.31 ± 0.88 degrees and 1.31 ± 0.88 degrees, respectively, compared to the HC group’s mean of 1.16 ± 0.43 degrees and 0.93 ± 0.50 degrees, respectively (Figure 3.3). In line with the hip and knee joints, sphericity was not assumed for the ankle joint range of motion at 0.33Hz, and while the Greenhouse-Geisser adjustment found a significant within-subject effect of

amplitude [$F(1.268,24.086) = 4.056, p = 0.047$] both interaction amplitude*group [$F(1.268,24.086) = 0.060, p = 0.863$] and between-subject [$F(1,19) = 0.003, p = 0.960$] effects were not significant.

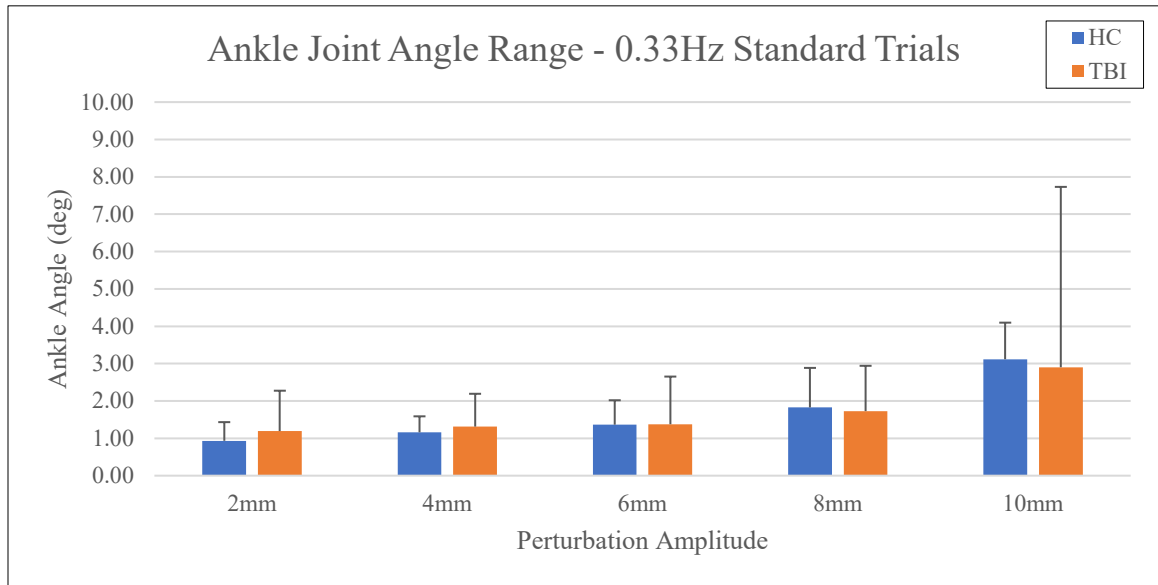


Figure 5.3. Mean ankle joint values for HC and TBI during perturbations delivered at 0.33Hz

The mean AP-ML COM path length for the 0.33Hz perturbations was larger for the HC group for three out of the five perturbation amplitudes and the TBI group's mean was higher for the remaining two perturbations. For the 10mm perturbation the HC group's mean path length was larger at 12.63 ± 4.10 mm while the TBI group's mean was 10.67 ± 6.43 mm, but for the 8mm perturbation the mean TBI group's mean AP-ML COM path length was larger at 8.57 ± 5.27 mm compared to the HC group's mean which was 7.87 ± 4.34 mm. The HC group's mean path length was larger than the TBI groups for both the 6 and 4mm perturbations, with their mean's coming in at 9.52 ± 3.88 mm and 8.25 ± 3.79 mm for the HC group vs 7.93 ± 3.85 mm and 7.97 ± 8.51 mm for the TBI group for the perturbation amplitudes, respectively. At 2mm the TBI group's mean path

length was larger at 6.76 ± 2.03 mm compared the HC group's which was 6.37 ± 4.81 mm (Figure 3.3). The Greenhouse-Geisser adjustment was not necessary for the AP-ML COM path length at 0.33Hz as sphericity could be safely assumed, and the within-subject effect of amplitude [$F(4.000,76.000) = 2.882, p = 0.028$] was found to be significant, while both the interaction effect of amplitude*group [$F(4.000,76.000) = 0.291, p = 0.883$] and the between-subject effect [$F(1.000,19.000) = 0.248, p = 0.624$] were not found to be significant.

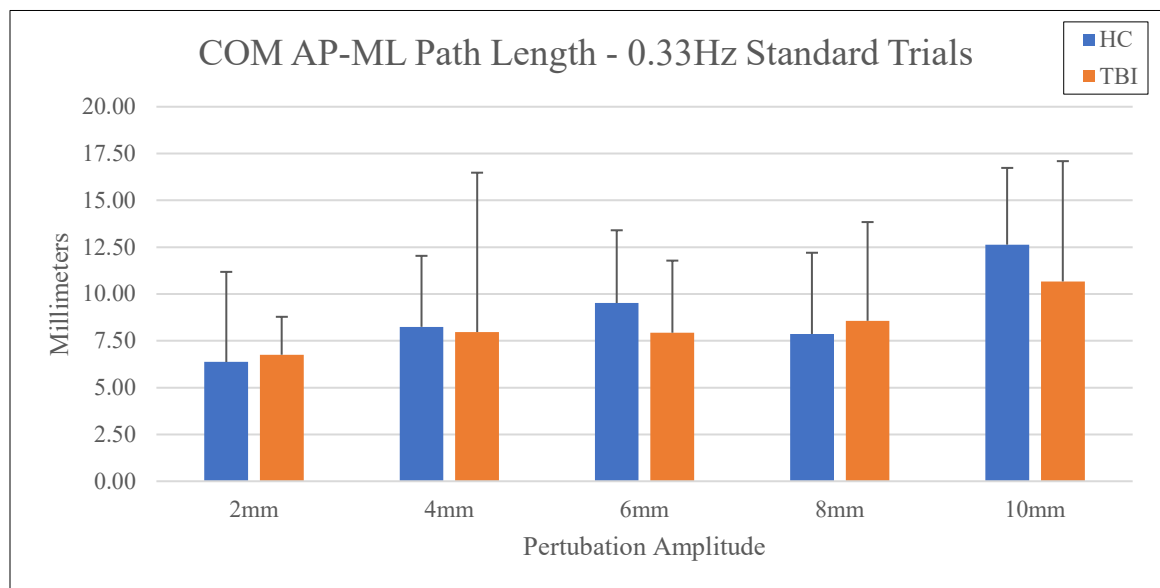


Figure 5.4. Mean AP-ML COM path length values for HC and TBI during perturbations delivered at 0.33Hz

Analogous to the mean AP-ML COM path length, the mean AP-ML COM average velocity for the 0.33Hz perturbations was larger for the HC group for three out of the five perturbation amplitudes and the TBI group's mean was higher for the remaining two perturbations. For the 10mm perturbation the HC group's mean average velocity was larger at 2.11 ± 0.68 mm/s while the TBI group's mean was 1.78 ± 1.07 mm/s, but for the 8mm perturbation the mean TBI group's mean AP-ML COM average velocity was larger

at 1.43 ± 0.88 mm/s compared to the HC group's mean which was 1.31 ± 0.72 mm/s. The HC group's mean average velocity was larger than the TBI groups for both the 6 and 4mm perturbations, with their mean's coming in at 1.59 ± 0.65 mm/s and 1.37 ± 0.65 mm/s for the HC group vs 1.32 ± 0.64 mm/s and 1.33 ± 1.42 mm/s for the TBI group for the perturbation amplitudes, respectively. At 2mm the TBI group's mean average velocity was larger at 1.13 ± 0.34 mm/s compared the HC group's which was 1.06 ± 0.80 mm/s (Figure 3.5). Sphericity was safely assumed for the mean AP-ML COM average velocity at 0.33Hz, with significant within-subject effect being found for amplitude [$F(4.000,76.000) = 2.889, p = 0.028$], but not such significance was found for amplitude*group [$F(4.000,76.000) = 0.289, p = 0.884$] or between-subjects [$F(1.000,19.000) = 0.246, p = 0.625$] effects.

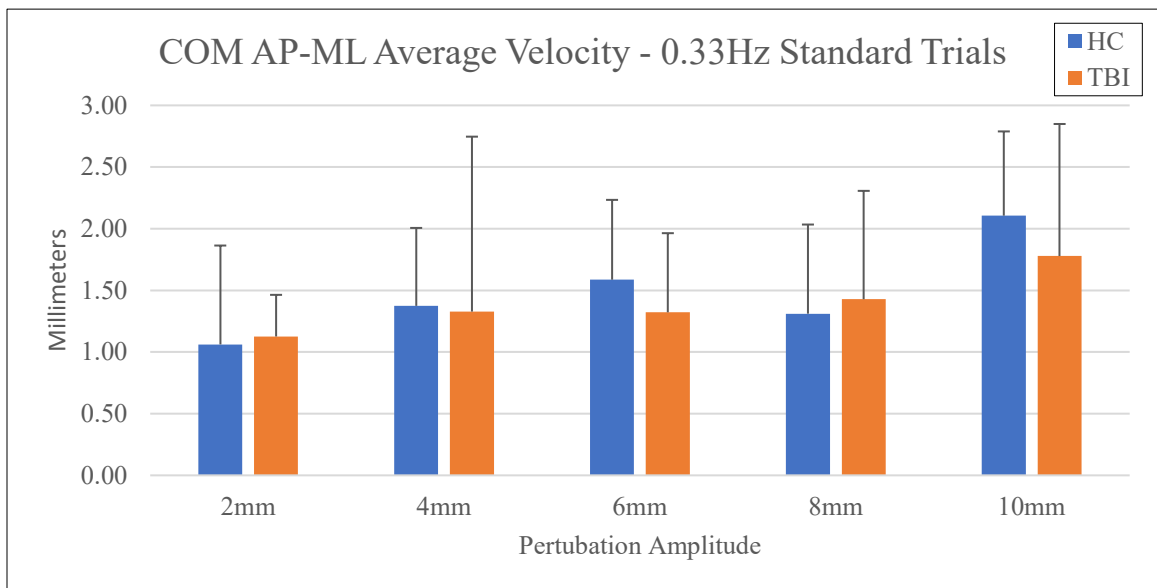


Figure 5.5. Mean AP-ML COM average velocity values for HC and TBI during perturbations delivered at 0.33Hz

The mean AP COM range for the 0.33Hz perturbations was larger for the HC group for three out of the five perturbation amplitudes and the TBI group's mean was

higher for the remaining two perturbations. For the 10mm perturbation the HC group's mean range was larger at 31.08 ± 7.16 mm while the TBI group's mean was 29.10 ± 13.95 mm, but for the 8mm perturbation the mean TBI group's mean AP COM range was larger at 20.72 ± 5.64 mm compared to the HC group's mean which was 17.01 ± 3.84 mm. The HC group's mean range was larger than the TBI groups for both the 6 and 4mm perturbations, with their mean's coming in at 19.40 ± 5.24 mm and 16.61 ± 4.52 mm for the HC group vs 19.08 ± 6.00 mm and 16.26 ± 8.43 mm for the TBI group for the perturbation amplitudes, respectively. The TBI group's mean range for the 2mm perturbation was larger at 13.49 ± 5.34 mm compared the HC group's which was 10.87 ± 3.94 mm (Figure 3.6). Sphericity could not be assumed for AP COM range at 0.33Hz, but a significant within-subject effect of amplitude [$F(2.479,47.110) = 22.894, p < 0.001$] was found after the Greenhouse-Geisser adjustment was applied. No significance was found for either the interaction amplitude*group effect [$F(2.479,47.110) = 0.715, p = 0.523$] or between-subject group effect [$F(1.000,19.000) = 0.129, p = 0.724$] effects.

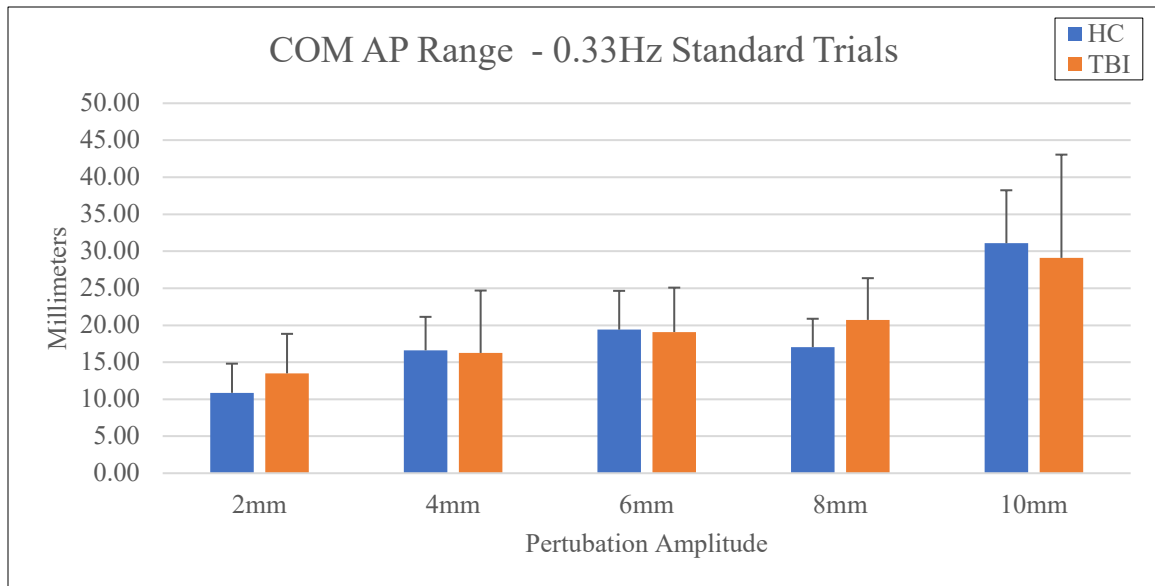


Figure 5.6. Mean AP COM range values for HC and TBI during perturbations delivered at 0.33Hz

The TBI group's mean AP-ML COP path length was larger than the HC group's mean for four out of five perturbations at 0.33Hz, with the HC group's mean only being larger at 10mm coming in at 30.73 ± 9.99 cm compared to the TBI group's mean of 28.70 ± 19.83 cm. For the remaining perturbations at 8, 6, 4, and 2mm the TBI group's mean path lengths were larger as their means decreasing with amplitude coming in at 25.63 ± 16.19 cm, 21.09 ± 15.91 cm, 21.09 ± 15.91 cm, and 18.00 ± 16.01 cm, respectively, while the HC group's mean values followed a similar pattern but were smaller at 16.65 ± 3.71 cm, 14.73 ± 1.90 cm, 12.06 ± 2.04 cm, and 9.80 ± 1.95 cm, respectively (Figure 5.7). Mauchly's test indicated that sphericity could not be assumed for AP-ML COP path length at 0.33Hz necessitating the use of the Greenhouse-Geisser adjustment, after which a significant within-subject effect of amplitude was found [$F(1.269,24.120) = 12.137$, $p = 0.001$], while neither the interaction effect of amplitude*group [$F(1.269,24.120) = 1.615$, $p = 0.220$] or the between-subject effect [$F(1.000,19.000) = 1.456$, $p = 0.242$] were significant.

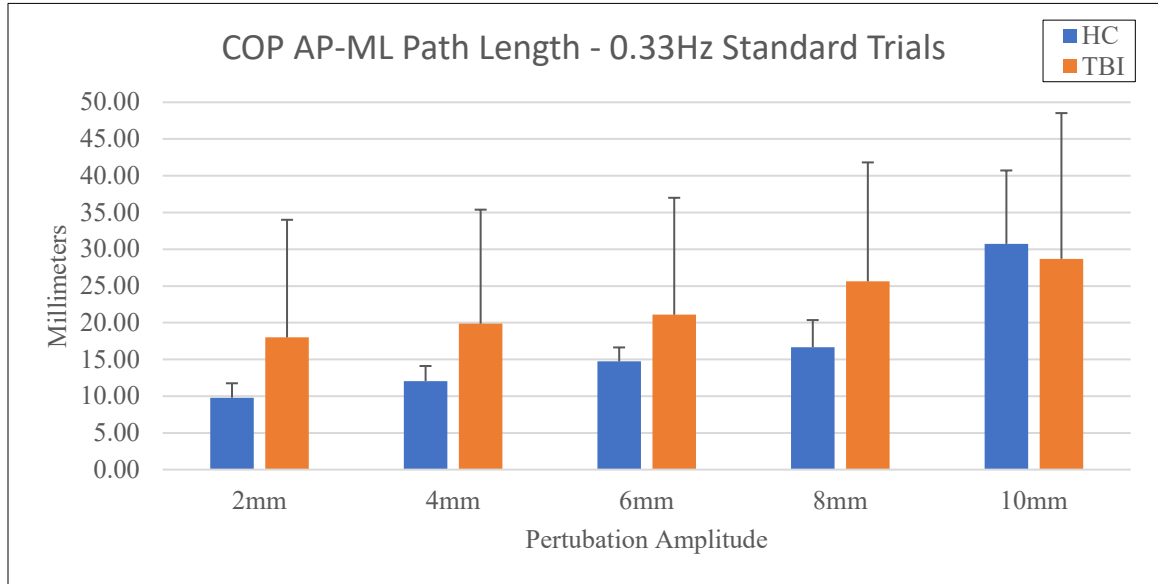


Figure 5.7. Mean AP-ML COP path length values for HC and TBI during perturbations delivered at 0.33Hz

AP-ML COP average velocity followed a similar pattern to AP-ML COP path length where the TBI group’s means were larger than the HC group’s mean for four out of five perturbations at 0.33Hz, with the HC group’s mean only being larger at 10mm coming in at 5.12 ± 1.67 cm compared to the TBI group’s mean of 4.78 ± 3.31 cm. The TBI group’s mean average velocities were larger for the remaining 8, 6, 4, and 2mm perturbations with their means decreasing with perturbation amplitude resulting in 4.27 ± 2.70 cm/s, 3.51 ± 2.65 cm/s, 3.31 ± 2.59 cm/s, and 3.00 ± 2.67 cm/s, respectively, while the HC group’s mean values followed a similar pattern but were smaller at 2.77 ± 0.62 cm/s, 2.45 ± 0.32 cm/s, 2.01 ± 0.34 cm/s, and 1.63 ± 0.33 cm/s, respectively (Figure 5.8). Once again, Mauchly’s test indicated that sphericity could not be assumed for AP-ML COP average velocity at 0.33Hz, and after the application of the Greenhouse-Geisser adjustment a significant within-subject effect of amplitude was found [$F(1.269,24.109) = 12.133$, $p = 0.001$], but neither the interaction effect of amplitude*group [$F(1.269,24.109)$

= 1.610, p = 0.220] or the between-subject [F(1.000,19.000) = 1.456, p = 0.242] effect were found to be significant .

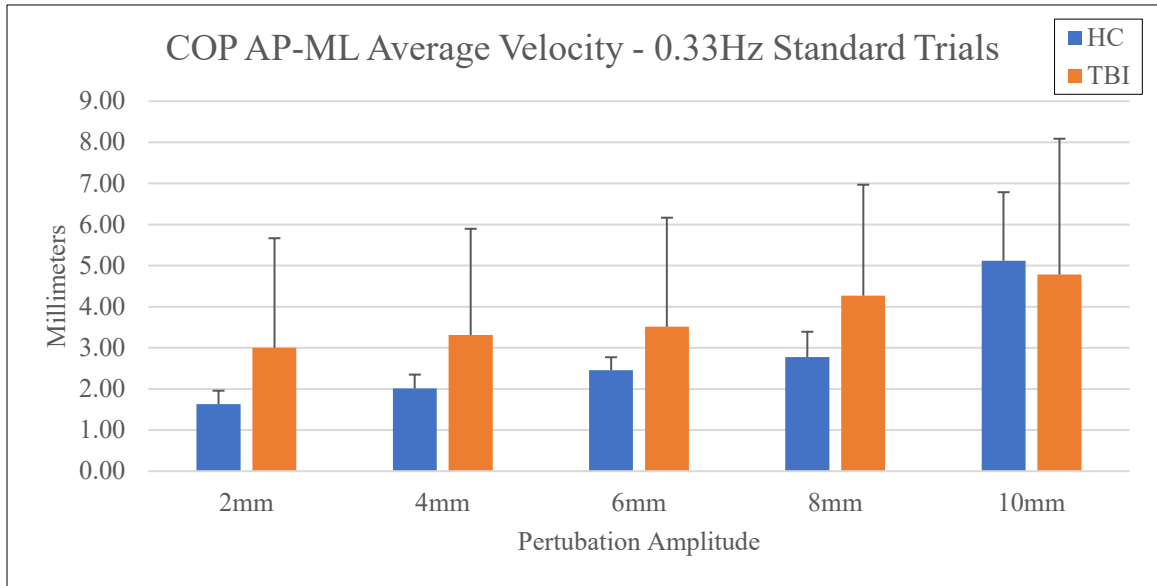


Figure 5.8. Mean AP-ML COP average velocity values for HC and TBI during perturbations delivered at 0.33Hz

The HC group’s mean AP COP range was larger than the TBI group’s mean range for two out of five perturbation amplitudes at 0.33Hz compared to only one perturbation for the previous two COP metrics. Initially continuing the same pattern as the earlier metrics, the TBI group’s mean for the 10mm perturbation was larger at 4.75 ± 4.55 cm compared to the HC group’s mean which was 6.96 ± 2.15 cm, while the HC group’s mean was smaller for 8mm at 3.23 ± 0.80 cm compared to the TBI group’s 3.75 ± 2.51 cm. The 6mm perturbation then bucked the trend with the HC group’s mean AP COP range being larger at 2.90 ± 0.59 cm compared to the TBI group’s mean of 2.83 ± 1.88 cm. For the remaining two perturbations of 4 and 2mm, the TBI groups means were larger coming in at 2.63 ± 2.19 cm and 2.19 ± 1.58 cm while to the HC group’s means were 2.55 ± 0.54 cm and 1.82 ± 0.41 cm, respectively (Figure 3.9). Sphericity was not

assumed for AP COP range at 0.33Hz and application of the Greenhouse-Geisser adjustment found a significant within-subjects effect of amplitude [$F(1.390,26.414) = 21.032, p < 0.001$], but once again did not find a significant effect for the interaction amplitude*group [$F(1.390,26.414) = 2.910, p = 0.088$] or between-subjects [$F(1.000,19.000) = 0.110, p = 0.743$].

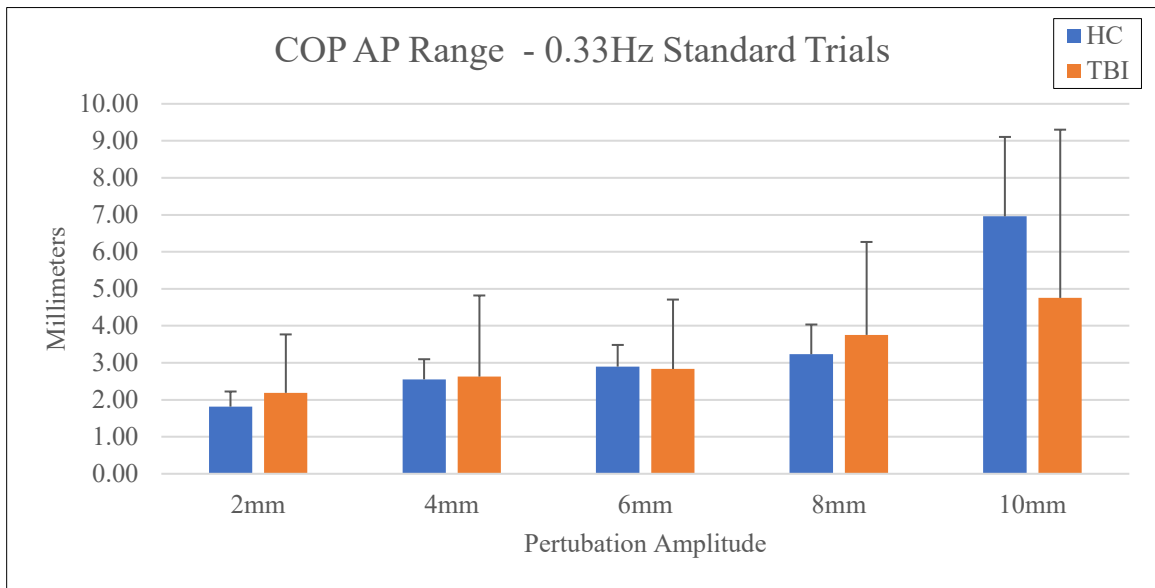


Figure 5.9. Mean AP COP range values for HC and TBI during perturbations delivered at 0.33Hz

Perturbations Delivered at 0.5 Hz

The TBI group's mean hip range of motion was larger than the HC group's mean for three out of the five perturbations at 0.5Hz. For the 10mm perturbation TBI group's mean was larger at 2.74 ± 1.73 degrees compared to the HC group's which was 2.08 ± 1.06 degrees, and this held true at 8mm as well as the TBI group's mean was 2.02 ± 1.54 degrees compared to the HC group's smaller mean of 1.36 ± 0.99 degrees. Conversely, the HC group's mean was larger for the 6mm perturbation; coming in at 1.57 ± 1.19 degrees compared to the TBI group's mean at 1.26 ± 0.59 degrees. The TBI group's

mean hip range of motion was once again larger than the HC group's mean for the 4mm perturbation, being 1.41 ± 1.01 degrees vs 1.02 ± 0.59 degrees, respectively, though both group's means were very similar for the 2mm perturbation the HC group's mean was slightly larger at 1.33 ± 1.04 degrees compared to the TBI group's mean at 1.27 ± 1.21 degrees (Figure 3.10). Sphericity was not assumed for the range of motion about the hip at 0.5Hz, though a significant within-subject effect of amplitude [$F(2.822,53.620) = 5.042, p = 0.004$] was found after the Greenhouse-Geisser adjustment was applied, but significance was not found for either interaction amplitude*group [$F(2.822,53.620) = 1.024, p = 0.386$] or between-subjects [$F(1.000,19.000) = 0.620, p = 0.441$] effects.

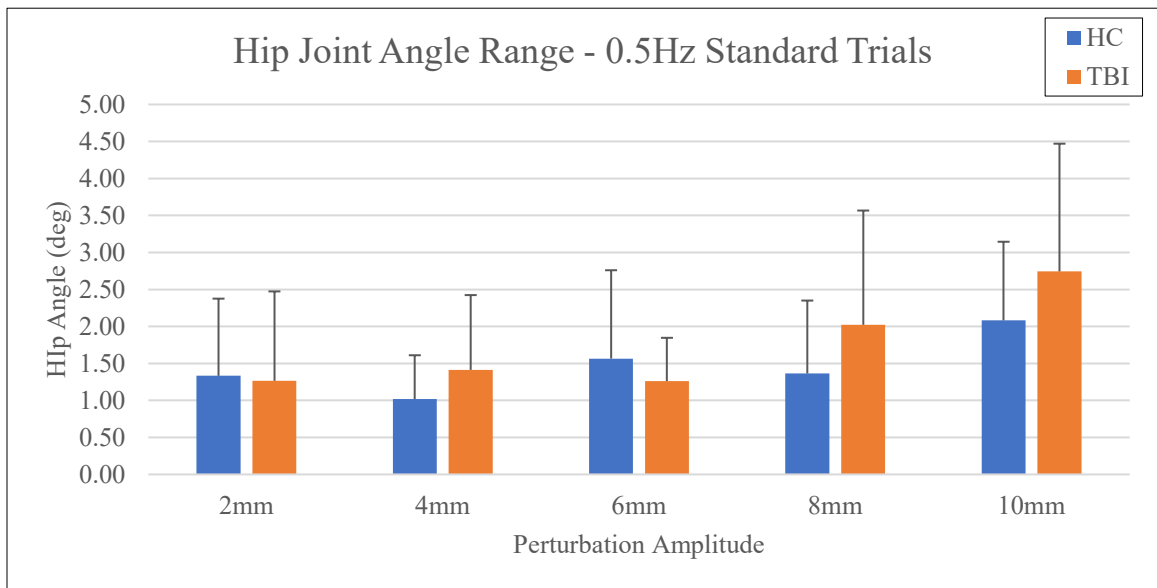


Figure 5.10. Mean hip joint angle range values for HC and TBI during perturbations delivered at 0.5Hz

The mean range of motion about the knee was larger for the HC group for three out of the five perturbation amplitudes at 0.5Hz. For the 10mm perturbation, the TBI group's mean was larger at 2.08 ± 1.39 degrees compared to the mean of the HC group which was 1.88 ± 1.29 degrees. Conversely, the HC group's mean was larger for both the

8 and 6mm amplitudes, coming in at 1.71 ± 1.07 degrees and 1.64 ± 1.60 degrees, respectively, compared to the TBI group's 1.61 ± 0.79 degrees and 1.28 ± 1.09 degrees, respectively. At 4mm the TBI group's mean knee range was larger at 1.15 ± 0.82 degrees compared to the HC group's mean which was 0.86 ± 0.44 degrees, though the HC group's mean was once again larger for the 2mm perturbation coming in at 1.30 ± 1.49 degrees compared to the TBI group's mean at 0.74 ± 0.53 degrees (Figure 3.11).

Sphericity was assumed for the range of motion about the knee at 0.5Hz, and the within-subject effect of amplitude [$F(4.000,76.000) = 5.337, p = 0.001$] was found to be significant while the effect of interaction amplitude*group [$F(4.000,76.000) = 1.003, p = 0.411$] and the effect of between-subject [$F(1.000,19.000) = 0.083, p = 0.776$] were not.

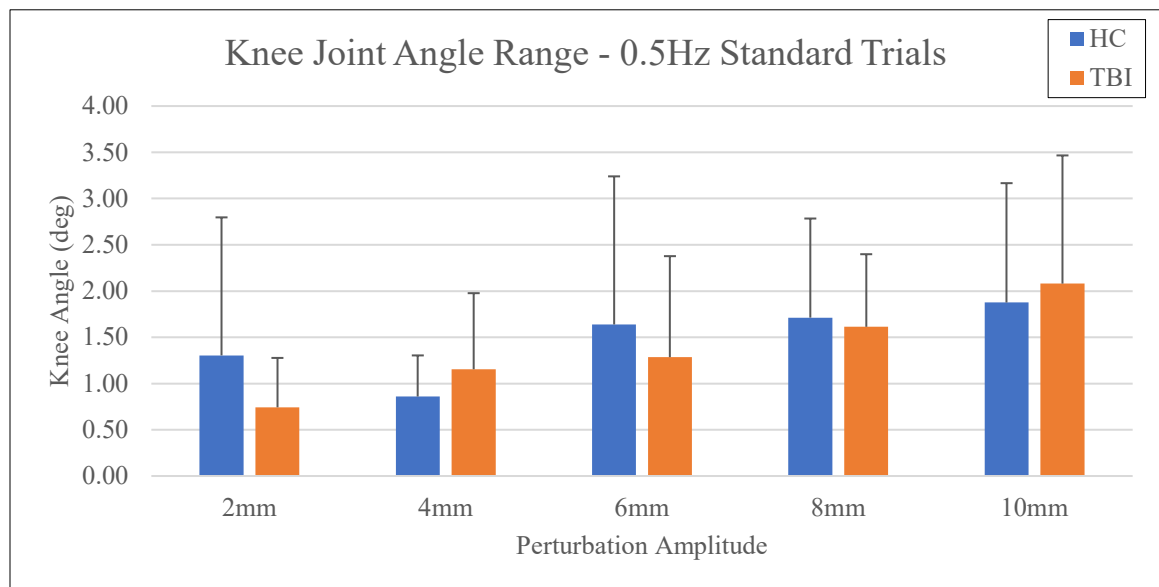


Figure 5.11. Mean knee joint angle range values for HC and TBI during perturbations delivered at 0.5Hz

The mean range of motion about the ankle at 0.5Hz was larger for the TBI group for two out of the five perturbation amplitudes, while the HC group's mean was larger for two of the remaining three amplitudes, and both group's means were essentially the same

for the final amplitude. The TBI group's mean range for the 10 and 8mm perturbation was larger than the HC groups, at 2.06 ± 1.60 degrees and 1.49 ± 0.43 degrees, respectively compared to 1.58 ± 0.63 degrees and 1.36 ± 0.53 degrees, respectively. The HC group's mean ankle range of 1.44 ± 0.98 degrees was larger than the TBI group's mean for the 6mm perturbation of 1.26 ± 0.65 degrees, but both group's means were very similar for the 4mm perturbation, coming in at 1.25 ± 0.55 degrees for the HC group and 1.27 ± 0.75 degrees for the TBI group. The HC group's mean ankle range was once again larger than the TBI groups for the 2mm perturbation, at 1.36 ± 1.52 degrees vs 0.89 ± 0.57 degrees, respectively (Figure 3.12). Sphericity was not assumed for the mean ankle range of motion at 0.5Hz and application of the Greenhouse-Geisser adjustment did not find any significant amplitude [$F(2.636,50.087) = 2.098, p = 0.120$] or amplitude*group [$F(2.636,50.087) = 0.956, p = 0.412$] interaction effects, or between-subject [$F(1.000,19.000) = 0.001, p = 0.977$] effects.

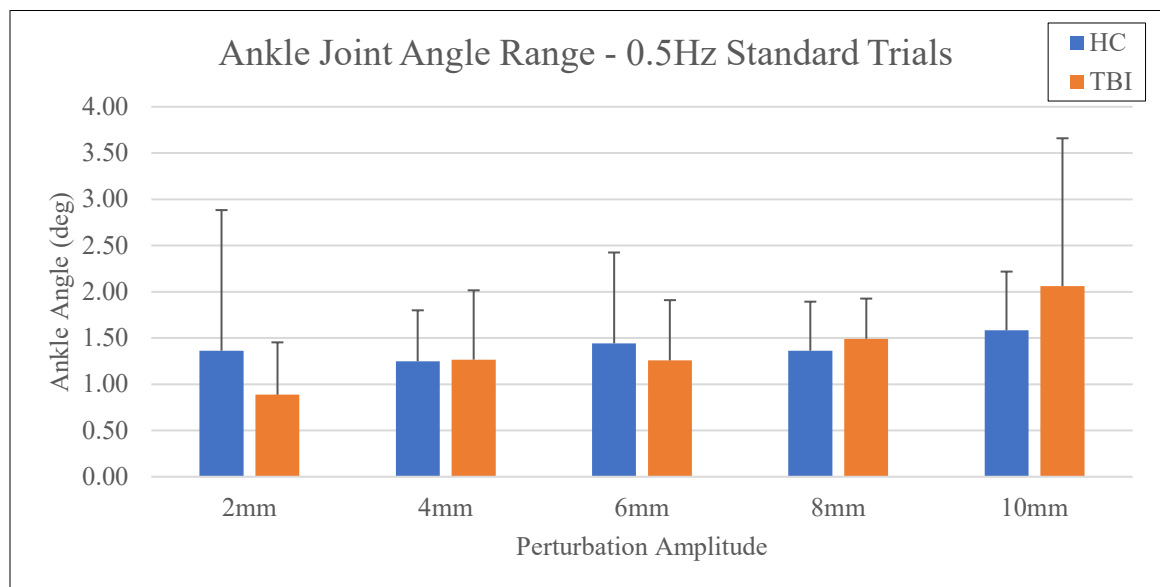


Figure 5.12. Mean ankle joint angle range values for HC and TBI during perturbations delivered at 0.5Hz

The AP-ML COM mean path length was larger for the TBI group for all perturbation amplitudes at 0.5Hz. The TBI group's mean for the 10mm perturbation was 11.44 ± 4.68 mm compared to 9.67 ± 3.12 mm for the HC group and came in at 11.88 ± 7.32 mm compared to 8.63 ± 1.83 mm for the 8mm perturbation. At 6mm, the TBI group's mean was 10.00 ± 7.89 mm compared to the HC group mean of 8.97 ± 4.58 mm, while their means were 11.07 ± 7.97 mm and 8.80 ± 5.03 mm, respectively for the 4mm perturbation, and 8.58 ± 6.42 mm vs 8.05 ± 5.61 mm, respectively for the 2mm perturbation (Figure 3.13). Sphericity was assumed for mean AP-ML COM path length at 0.5Hz, but no significant effects were found (amplitude: $[F(4.000,76.000) = 0.837, p = 0.506]$, amplitude*group $[F(4.000,76.000) = 0.129, p = 0.971]$, between-group $[F(1.000,19.000) = 1.550, p = 0.228]$).

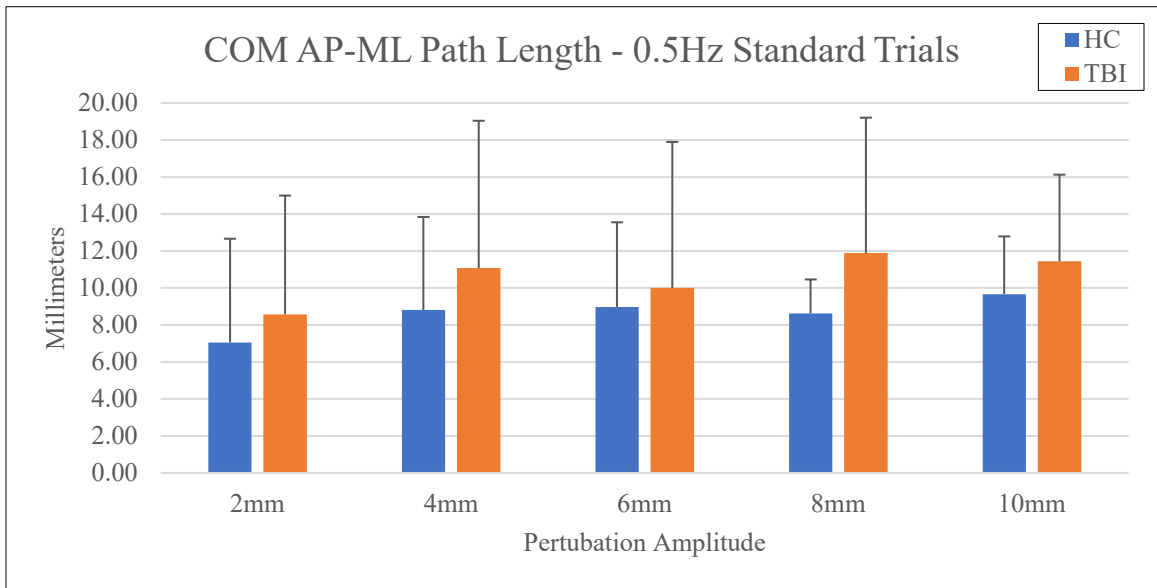


Figure 5.13. Mean AP-ML COM path length values for HC and TBI during perturbations delivered at 0.5Hz

Continuing the trend seen in the mean AP-ML path length, the TBI groups mean AP-ML Average Velocity was larger than the HC group's for all perturbation amplitudes

at 0.5Hz The TBI group's mean was 2.29 ± 0.94 mm/s compared to the HC group's mean of 1.93 ± 0.62 mm/s for the 10mm perturbation, 2.38 ± 1.46 mm/s vs 1.73 ± 0.37 mm/s at 8mm, and was 2.00 ± 1.58 mm/s compared to 1.79 ± 0.92 mm/s for 6mm. At 4mm, the TBI group's mean was 2.21 ± 1.59 mm/s compared to the HC group's which was 1.76 ± 1.01 mm/s, and for the 2mm perturbation, the TBI group's mean was 1.72 ± 1.28 mm/s vs the HC group's 1.41 ± 1.12 mm/s (Figure 3.14). Sphericity was assumed for mean AP-ML COM average velocity at 0.5Hz, however no significant effects were found (amplitude: $[F(4.000,76.000) = 0.840, p = 0.504]$, amplitude*group $[F(4.000,76.000) = 0.129, p = 0.971]$, between-group $[F(1.000,19.000) = 1.549, p = 0.228]$).

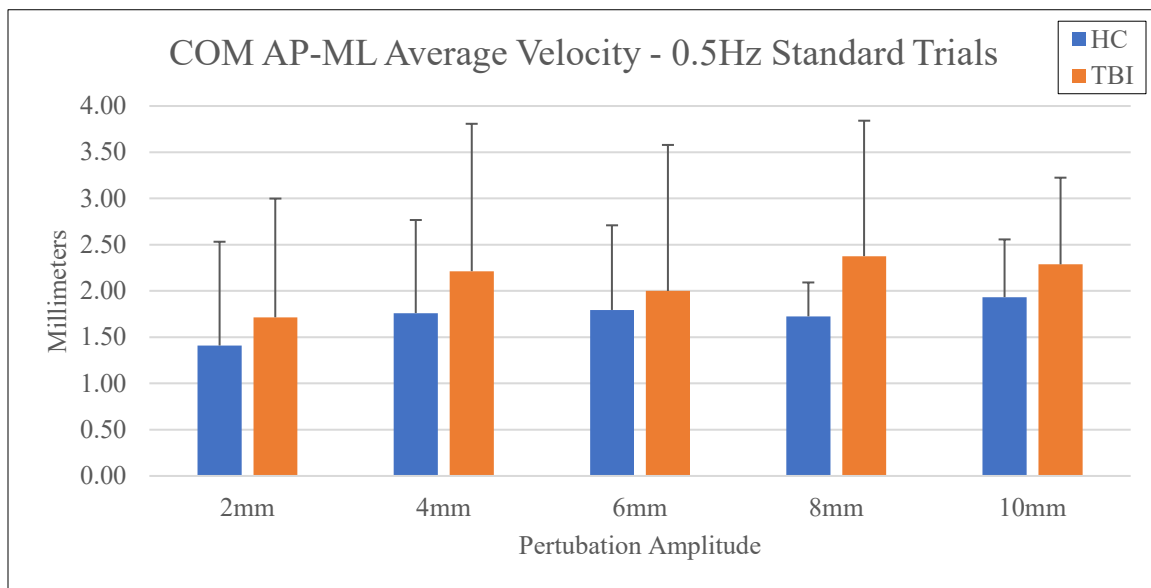


Figure 5.14. Mean AP-ML COM average velocity values for HC and TBI during perturbations delivered at 0.5Hz

The TBI group's mean AP COM range was larger than the HC group's mean for four out of the five perturbation amplitudes at 0.5Hz, in a departure from AP-ML COM path length and average velocity. For the 10mm perturbation, the TBI group's mean was larger at 27.14 ± 11.74 mm compared to 21.22 ± 5.28 mm for the HC group, and at 8mm

the TBI group's mean was 25.99 ± 10.37 mm vs the HC group's 22.62 ± 3.95 mm. The HC group's mean was larger for the 6mm perturbation than the TBI group's, coming in at 18.64 ± 4.07 mm and 18.04 ± 9.98 mm, respectively, but the TBI group's mean was larger for the 4 and 2mm perturbations, being 20.78 ± 12.03 mm and 15.00 ± 7.41 mm, respectively vs 16.40 ± 4.23 mm and 13.84 ± 8.88 mm, respectively for the HC group (Figure 3.15). Sphericity was safely assumed for AP COM range at 0.5Hz, and a significant within-subject effect of amplitude [$F(4.000,76.000) = 7.488, p < 0.001$] was found, but significance was not found for any other effects (amplitude*group [$F(4.000,76.000) = 0.697, p = 0.596$], between-group [$F(1.000,19.000) = 1.136, p = 0.300$]).

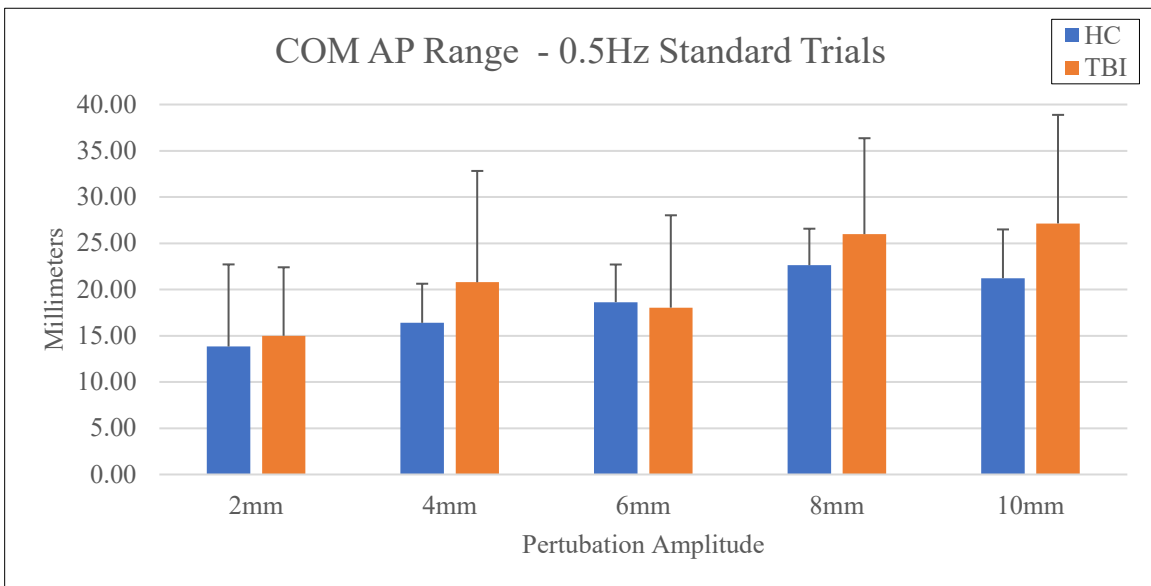


Figure 5.15. Mean AP COM range values for HC and TBI during perturbations delivered at 0.5Hz

The TBI group's mean AP-ML COP path length was larger than the HC group's mean for all perturbation amplitudes at 0.5Hz. The TBI group's mean was 26.34 ± 9.65 cm compared to the HC group's mean of 22.43 ± 70.07 cm for the 10mm perturbation,

and was 22.66 ± 10.43 cm vs 17.37 ± 6.29 cm for the 8mm perturbation. At 6mm, the TBI group's mean was 16.71 ± 7.13 cm compared to the HC group's mean which was 16.13 ± 5.64 cm, at 4mm their mean was 15.43 ± 7.35 cm vs 11.50 ± 4.53 cm, and for the 2mm perturbation, the TBI group's mean was 12.53 ± 5.73 cm vs 10.00 ± 3.40 cm for the HC group (Figure 3.16). Sphericity was assumed for AP-ML COP path length at 0.5Hz and a significant effect as found for within-subject factor of amplitude [$F(4.000,76.000) = 22.893, p < 0.001$], but no other significant effects were found (amplitude*group: [$F(4.000,76.000) = 0.666, p = 0.618$], between-subject [$F(1.000,19.000) = 1.663, p = 0.213$])

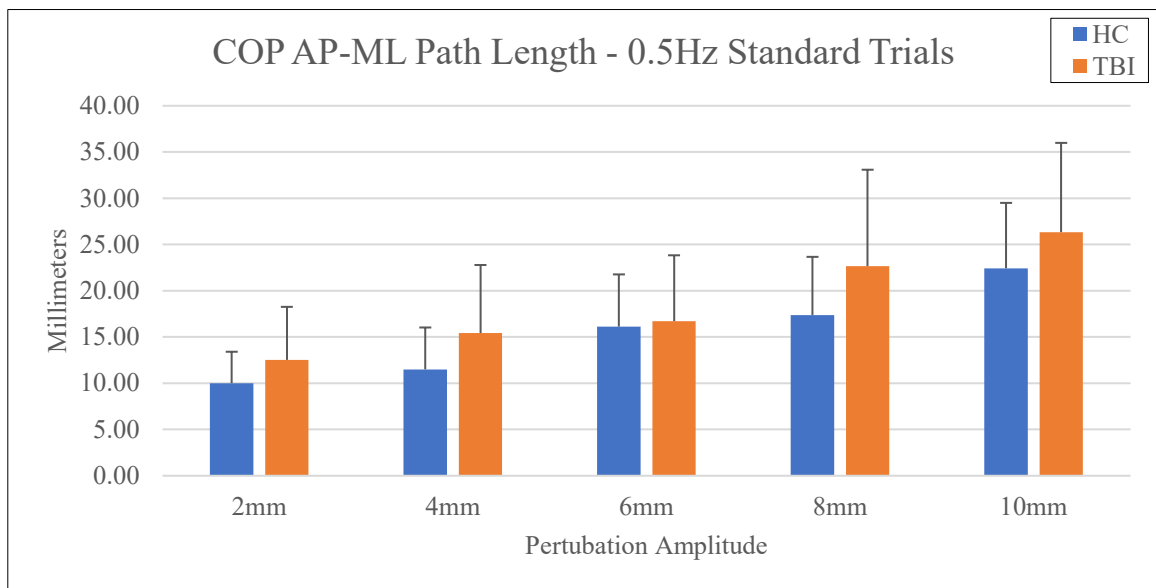


Figure 5.16. Mean AP-ML COP path length values for HC and TBI during perturbations delivered at 0.5Hz

The mean AP-ML COP average velocity for the TBI group was larger than the HC group's mean for all perturbation amplitudes at 0.5Hz, similar to AP-ML COP path length. The TBI group's mean was 5.27 ± 1.93 cm/s compared to the HC group's mean

of 4.49 ± 1.41 cm/s for the 10mm perturbation, and was 4.53 ± 2.09 cm/s vs 3.47 ± 1.26 cm/s for the 8mm perturbation. At 6mm, the TBI group's mean was 3.34 ± 1.43 cm/s compared to the HC group's mean which was 3.23 ± 1.13 cm/s, at 4mm their mean was 3.09 ± 1.47 cm/s vs 2.30 ± 0.91 cm/s, and for the 2mm perturbation, the TBI group's mean was 2.51 ± 1.15 cm/s vs 2.00 ± 0.68 cm/s for the HC group (Figure 3.17).

Sphericity was assumed for AP-ML COP average velocity at 0.5Hz and a significant effect as found for within-subject factor of amplitude [$F(4.000,76.000) = 22.894, p < 0.001$], but no other significant effects were found (amplitude*group: [$F(4.000,76.000) = 0.667, p = 0.617$], between-subject [$F(1.000,19.000) = 1.659, p = 0.213$])

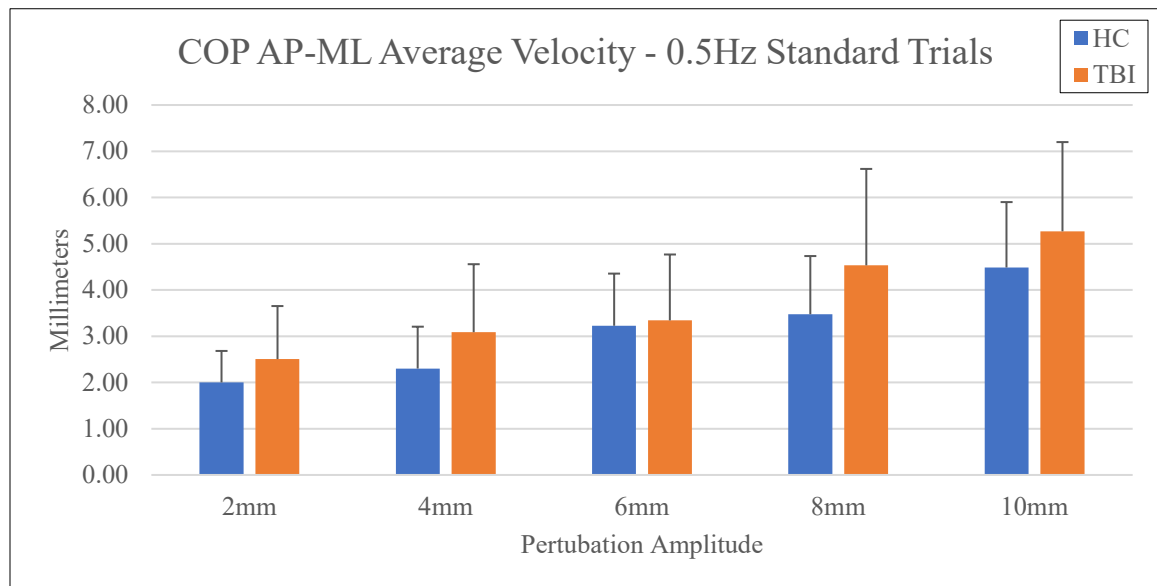


Figure 5.17. Mean AP-ML COP average velocity values for HC and TBI during perturbations delivered at 0.5Hz

Mean AP COP range was larger for the HC group for two out of the five perturbations at 0.5Hz, while it was larger for the TBI group for two of the remaining perturbation, and was essentially same for the final amplitude. The HC group's mean for the 10mm perturbation was 4.68 ± 1.45 cm, which was larger than the TBI group's mean

of 4.59 ± 2.44 cm, but the TBI group's mean was larger for the 8mm perturbation, coming in at 4.10 ± 3.05 cm compared to the HC group's 3.86 ± 1.15 cm. For the 6mm perturbation the HC groups mean AP COP range was once again larger at 3.64 ± 1.34 cm vs the TBI group's mean of 3.18 ± 2.21 cm, but the TBI group's mean was then larger for the 4mm perturbation as it was 3.05 ± 2.39 cm compared to the HC group's 2.63 ± 0.60 cm. Both group's mean AP COP ranges were essentially the same at 2mm, with the TBI group's being 2.23 ± 1.54 cm compared to 2.26 ± 1.43 cm for the HC group (Figure 3.18). Sphericity was assumed for AP COP range at 0.5Hz, and as was the case for both AP-ML COP path length and velocity, a significant effect as found for the within-subject factor of amplitude [$F(4.000,76.000) = 9.943, p < 0.001$], but no other significant effects were found (amplitude*group: [$F(4.000,76.000) = 0.315, p = 0.867$], between-subject [$F(1.000,19.000) = 0.000, p = 0.983$]).

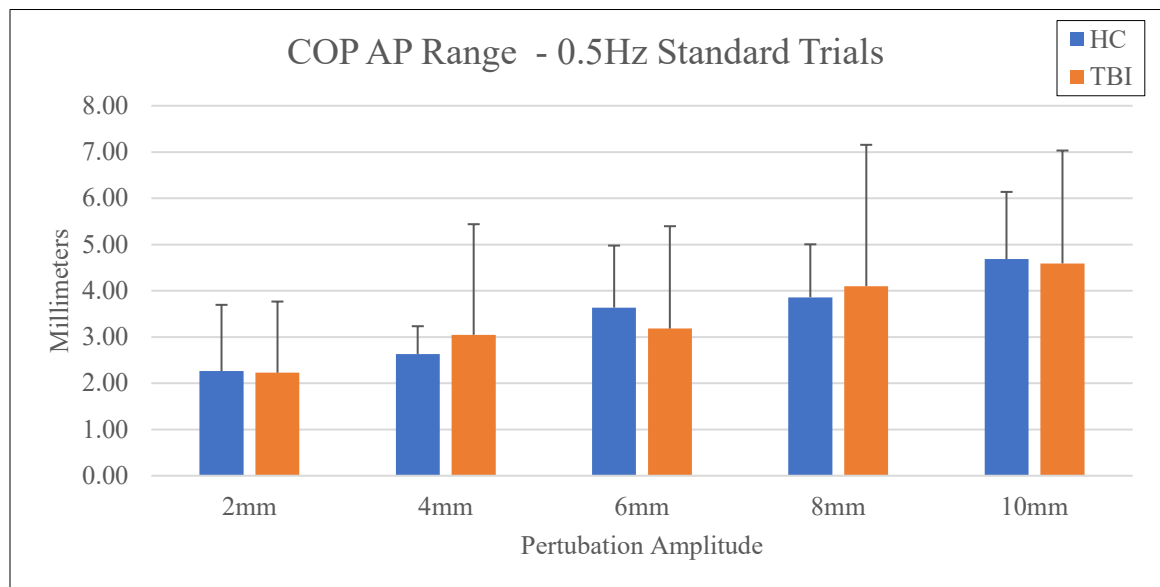


Figure 5.18. Mean AP COP range values for HC and TBI during perturbations delivered at 0.5Hz

Perturbations Delivered at 1.0 Hz

The mean range of motion about the hip joint was larger for the TBI group for three out of the five perturbations at 1.0Hz, was larger for the HC group for one perturbation, and was the same for both groups for the final perturbation. The TBI group's mean was larger for the 10 and 8mm perturbation amplitudes, coming in at 7.46 ± 7.51 degrees and 4.24 ± 3.35 degrees, respectively compared to 7.23 ± 4.01 degrees and 3.57 ± 1.29 degrees, respectively for the HC group. For the 6mm perturbation the HC group's mean was larger at 2.51 ± 0.92 degrees compared to the TBI group's mean which was 2.35 ± 0.87 degrees, and for the 4mm perturbation both group's means were essentially the same with the TBI group's mean being 1.98 ± 1.36 degrees while the HC group's mean was 1.98 ± 1.16 degrees. The TBI group's mean range about the hip for the 2mm perturbation was larger at 1.28 ± 0.65 degrees compared to the HC group at 1.11 ± 0.58 degrees (Figure 3.19). Sphericity was not assumed for the hip range of motion at 1.0Hz, and after Greenhouse-Geisser adjustment was applied, a significant effect of within-subject amplitude [$F(1.325,25.176) = 15.899, p < 0.001$] was found, though neither interaction amplitude*group [$F(1.325,25.176) = 0.065, p = 0.400$] or between-subject [$F(1.000,19.000) = 0.045, p = 0.834$] factors were significant.

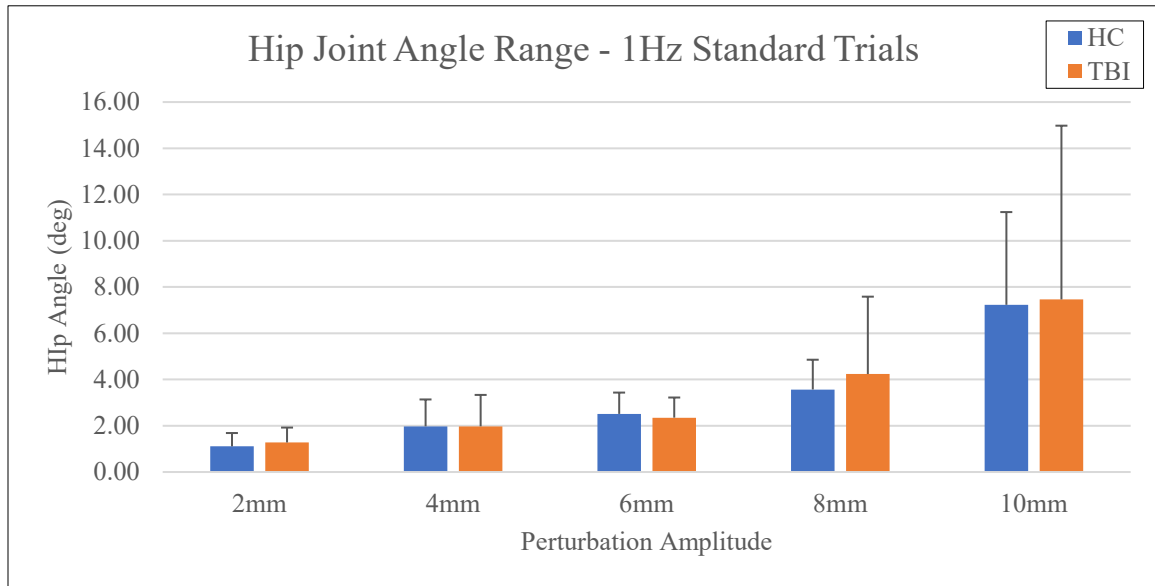


Figure 5.19. Mean hip joint angle range values for HC and TBI during perturbations delivered at 1.0Hz

The mean range of motion about the knee was larger for the HC group for four out of the five perturbations at 1.0Hz and was essentially the same for the remaining perturbation. The HC group’s mean knee range of motion for the 10mm perturbation was 8.57 ± 5.03 degrees compared to the TBI group’s mean of 6.92 ± 4.80 degrees, and at 8mm their mean was 5.40 ± 3.68 degrees vs the TBI group’s 2.85 ± 1.67 degrees. For the 6 and 4mm perturbations, the HC group’s means were 3.44 ± 3.00 degrees and 2.32 ± 1.95 degrees, respectively compared to the TBI group’s means of 1.86 ± 0.70 degrees and 1.86 ± 0.70 degrees, respectively. The TBI group’s mean for the 2mm perturbation was 1.13 ± 0.57 degrees, which was very similar to the HC group’s mean of 1.09 ± 0.55 degrees (Figure 3.20). Sphericity was not assumed for mean knee range of motion at 1.0Hz and after applying the Greenhouse Geisser adjustment, the within-subjects effect of amplitude [$F(1.648,31.304) = 25.796, p < 0.001$] was found to be significant, though no other significant effects were found (amplitude*group: [$F(1.648,31.304) = 0.896, p = 0.400$], between-subject: [$F(1.000,19.000) = 2.751, p = 0.114$]).

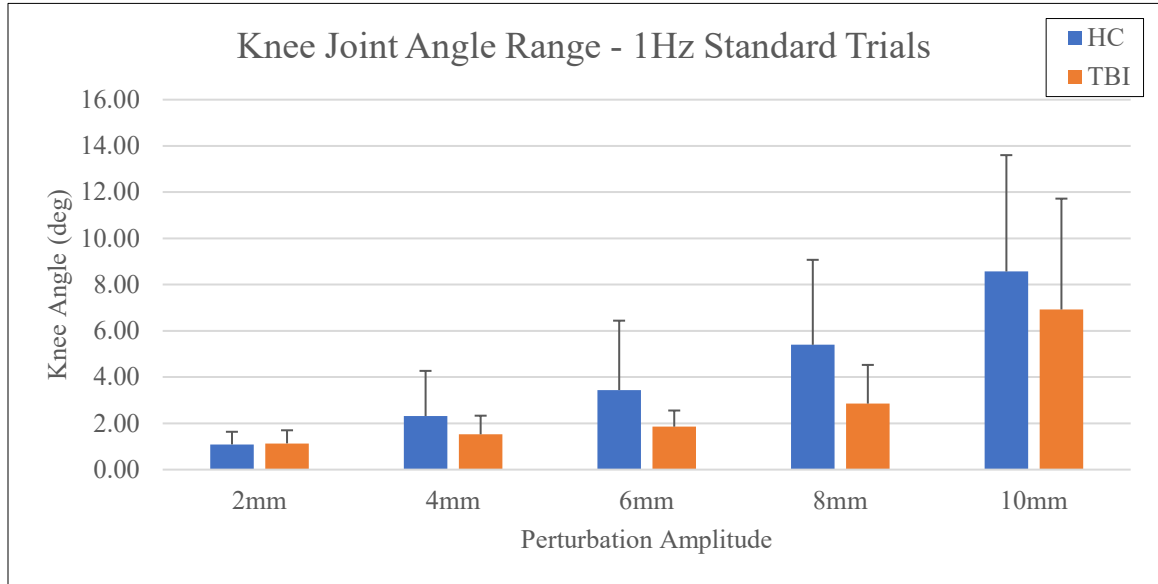


Figure 5.20. Mean knee joint angle range values for HC and TBI during perturbations delivered at 1.0Hz

The mean range of motion about the ankle for the 1.0Hz perturbations was larger for the HC group for four out of the five perturbation amplitudes, and was same as the TBI group for the remaining amplitudes. The HC group’s means for the 10 and 8mm perturbations were 5.37 ± 1.56 degrees and 3.90 ± 1.75 degrees, while the TBI group’s means were 4.97 ± 2.65 degrees and 2.62 ± 1.39 degrees, respectively. For the 6mm perturbation, the HC group’s mean range was 2.84 ± 1.24 degrees vs 1.62 ± 0.54 degrees for the TBI group, and for the 4mm perturbation, the HC group’s mean came in at 2.32 ± 1.29 degrees compared to the TBI group’s mean of 1.47 ± 0.57 degrees. The mean ankle range of motion for both groups was practically the same for the 2mm perturbation, with the TBI group’s mean being 1.22 ± 0.49 degrees and the HC group’s being 1.22 ± 0.41 degrees (Figure 3.21). Sphericity was not assumed for the mean ankle range of motion at 1.0Hz, and after the Greenhouse-Geisser adjustment was employed the within-subject effect of amplitude [$F(1.965,37.331) = 31.341, p < 0.001$] was found to be significant,

and while the within-subject effect of amplitude*group [$F(1.965,37.331) = 0.985, p = 0.382$] was not significant, and significant between-subject [$F(1.000,19.000) = 4.490, p = 0.048$] effect was found. Independent sample t-tests were performed, and after applying the Bonferroni correction for multiple comparison significance was set at $p < 0.01$, resulting in the 6mm perturbation about the ankle being found as significant at $p = 0.007$.

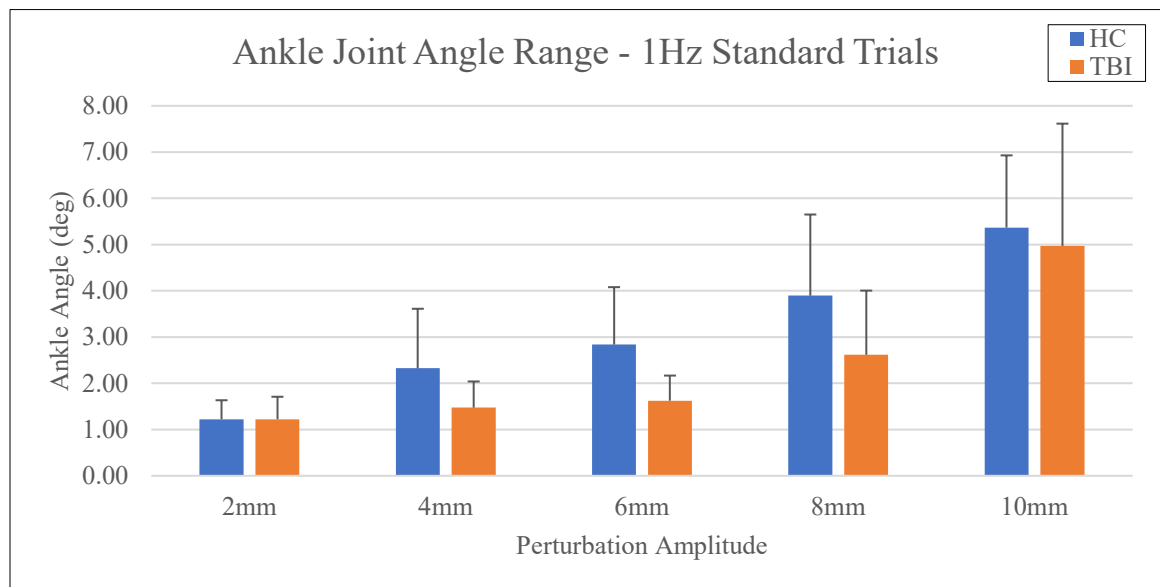


Figure 5.21. Mean ankle joint angle range values for HC and TBI during perturbations delivered at 1.0Hz

The mean AP-ML COM path length was larger for the HC group for three of the five perturbation amplitudes at 1.0Hz and was large for the TBI group for the remaining two amplitudes. The TBI group's mean for the 10mm perturbation was 16.05 ± 6.45 mm compared to the HC group's mean of 14.66 ± 6.45 mm. The HC group's means were larger for the 8, 6, and 4mm perturbations coming in at 13.26 ± 7.18 mm, 15.04 ± 8.65 mm, and 12.69 ± 6.38 mm, respectively compared to the TBI group's means of 10.93 ± 4.06 mm, 12.26 ± 6.33 mm, and 10.66 ± 5.42 mm, respectively. For the 2mm perturbation, the TBI group's mean was larger at 7.51 ± 4.50 mm compared to the HC

group's mean of 6.43 ± 2.52 mm (Figure 3.22). Sphericity was assumed for AP-ML COM path length at 1.0Hz, and a significant within-subject effect of amplitude [$F(4.000,76.000) = 6.494, p < 0.001$] was found, though no other significant effects were found ([$F(3.241,76.000) = 0.659, p = 0.592$], [$F(1.000,19.000) = 0.438, p = 0.516$]).

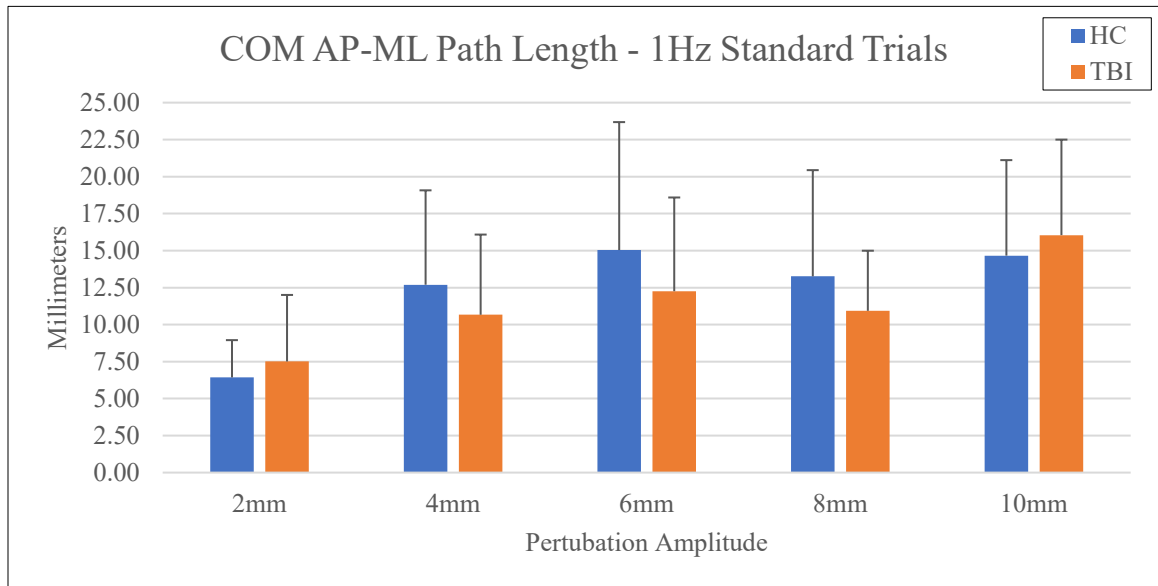


Figure 5.22. Mean AP-ML COM path length values for HC and TBI during perturbations delivered at 1.0Hz

The TBI group's mean AP-ML COM average velocity was larger for two out of the five perturbation amplitudes at 1.0Hz, and the HC group's mean was larger for the remaining three amplitudes. The TBI group's mean for the 10mm perturbation was 3.21 ± 1.29 mm/s compared to the HC group's 2.93 ± 1.29 mm/s. The HC group's means for the 8, 6, and 4mm perturbations were 2.65 ± 1.44 mm/s, 3.01 ± 1.73 mm/s, and 2.54 ± 1.28 mm/s, respectively vs 2.19 ± 0.81 mm/s, 2.45 ± 1.27 mm/s, and 2.13 ± 1.08 mm/s, respectively for the TBI group. For the 2mm perturbation, the TBI group's mean was 1.50 ± 0.90 mm/s compared to 1.29 ± 0.50 mm/s for the HC group (Figure 3.23).

Sphericity was assumed for mean AP-ML COM average velocity at 1.0Hz, and while a

significant within-subject effect of amplitude [$F(4.000,76.000) = 6.494, p < 0.001$] was found, neither interaction amplitude*group [$F(3.242,76.000) = 0.660, p = 0.591$] or between-subjects [$F(1.000,19.000) = 0.440, p = 0.515$] effects were significant.

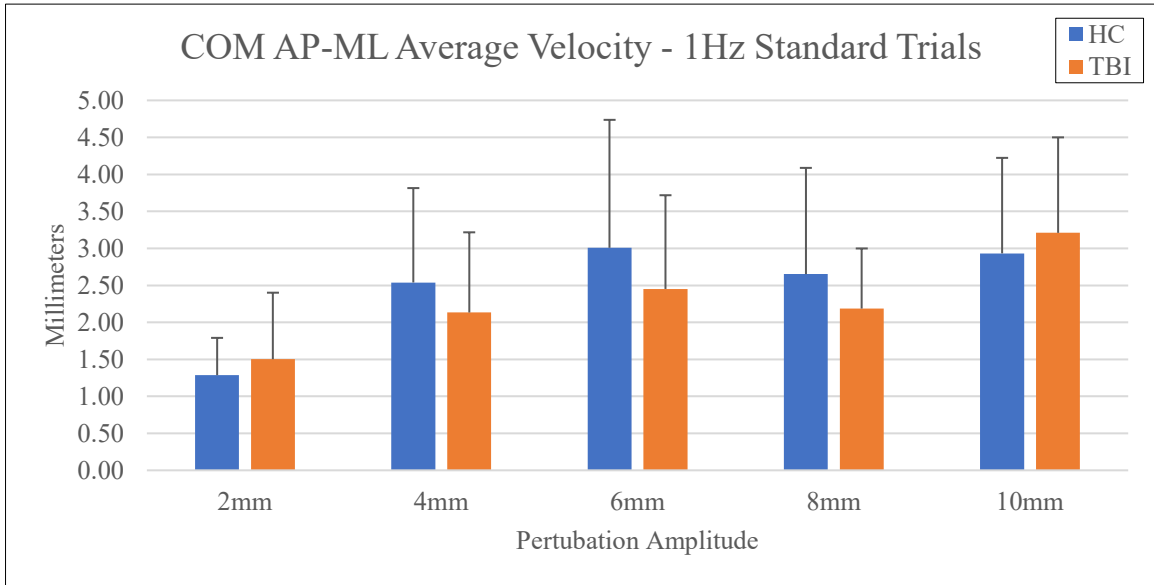


Figure 5.23. Mean AP-ML COM average velocity values for HC and TBI during perturbations delivered at 1.0Hz

The TBI group's mean AP COM range was larger for three out of the five perturbations amplitudes at 1.0Hz, and the HC group's mean was larger for the remaining two amplitudes. For the 10mm perturbation, the TBI group's mean was 35.35 ± 13.54 mm compared to the HC group's mean of 30.36 ± 9.06 mm, and their mean was 29.59 ± 5.72 mm for the 8mm perturbation vs 22.67 ± 7.35 mm for the HC group. The HC group's means for the 6 and 4mm perturbations were 29.59 ± 5.72 mm and 21.36 ± 7.63 mm, respectively vs 22.40 ± 8.71 mm and 19.18 ± 8.54 mm, respectively for the TBI group. The mean AP COM range for TBI group was 15.96 ± 6.65 mm for the 2mm perturbation compared to 15.47 ± 4.49 mm for the HC group (Figure 3.24). Sphericity was assumed for mean AP COM range at 1.0Hz, and while a significant within-subject

effect of amplitude [$F(4.000,76.000) = 11.612, p < 0.001$] was found, neither interaction amplitude*group [$F(2.775,76.000) = 1.389, p = 0.257$] or between-subjects [$F(1.000,19.000) = 0.175, p = 0.680$] effects were significant.

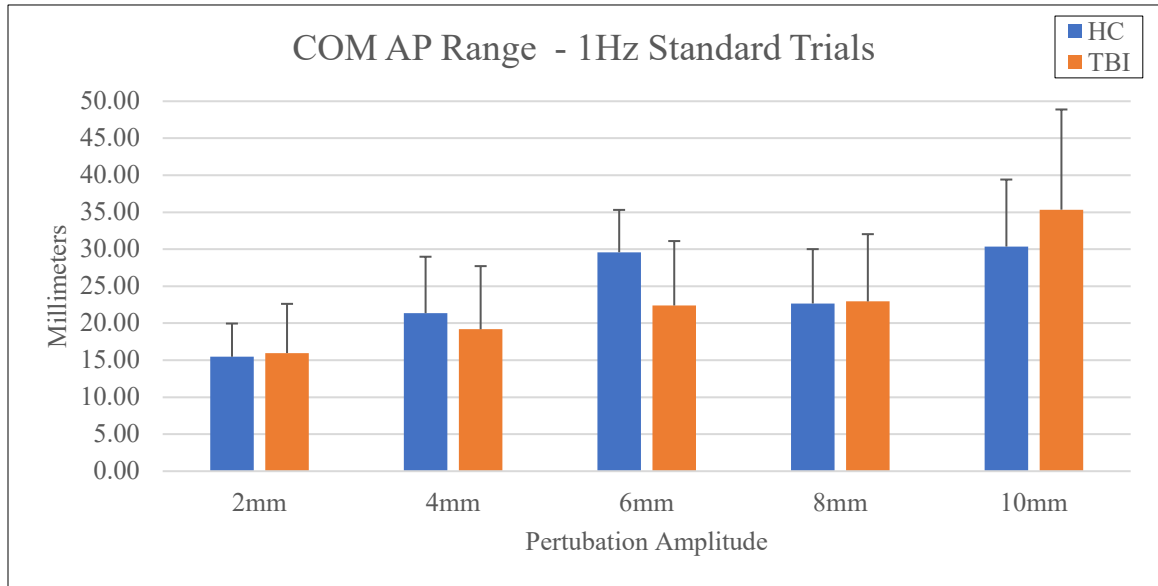


Figure 5.24. Mean AP COM range values for HC and TBI during perturbations delivered at 1.0Hz

The TBI group’s mean AP-ML COP path length was larger than the HC group’s for all perturbation amplitudes at 1.0Hz. For the 10mm perturbation, the TBI group’s mean was 71.64 ± 34.96 cm compared 68.20 ± 30.34 cm for the HC group, and was 48.32 ± 33.74 cm vs 37.63 ± 21.58 cm for the 8mm perturbation. The TBI group’s mean for the 6mm perturbation was 35.13 ± 18.66 cm compared to 30.36 ± 12.42 cm for the HC group, 28.11 ± 16.61 cm vs 25.06 ± 12.50 cm for the 4mm perturbation, and was 21.21 ± 13.33 cm compared to 14.71 ± 6.31 cm for the 2mm perturbation, respectively (Figure 3.25). Sphericity was not assumed for the AP-ML COP path length at 1.0Hz, though a significant within-subject effect of amplitude [$F(1.420,26.985) = 47.112, p < 0.001$] was found after application of the Greenhouse-Geisser adjustment, not other

effects were significant (amplitude: $[F(1.420,26.985) = 0.283, p = 0.680]$, between-subject: $[F(1.000,19.000) = 0.447, p = 0.512]$).

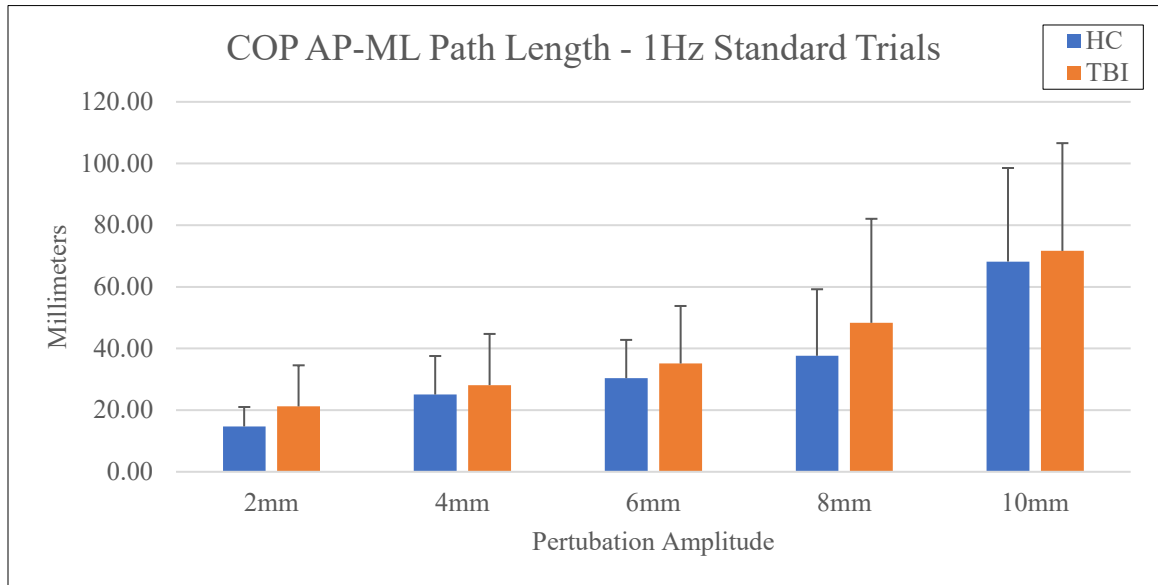


Figure 5.25. Mean AP-ML COP path length values for HC and TBI during perturbations delivered at 1.0Hz

The TBI group’s mean AP-ML COP average velocity was larger than the HC group’s for all perturbation amplitudes at 1.0Hz. For the 10mm perturbation, the TBI group’s mean was 14.33 ± 6.99 cm/s compared 13.64 ± 6.07 cm/s for the HC group, and was 9.66 ± 6.75 cm/s vs 7.53 ± 4.32 cm/s for the 8mm perturbation. The TBI group’s mean for the 6mm perturbation was 7.03 ± 3.73 cm/s compared to 7.03 ± 3.73 cm/s for the HC group, 5.62 ± 3.32 cm/s vs 5.01 ± 2.50 cm/s for the 4mm perturbation, and was 4.24 ± 2.67 cm/s compared to 2.94 ± 1.26 cm/s for the 2mm perturbation, respectively (Figure 3.26). Sphericity was not assumed for the AP-ML COP path length at 1.0Hz, though a significant within-subject effect of amplitude $[F(1.420,26.985) = 47.119, p < 0.001]$ was found after application of the Greenhouse-Geisser adjustment, not other effects were

significant (amplitude: $[F(1.420,26.985) = 0.283, p = 0.680]$, between-subject: $[F(1.000,19.000) = 0.448, p = 0.511]$).

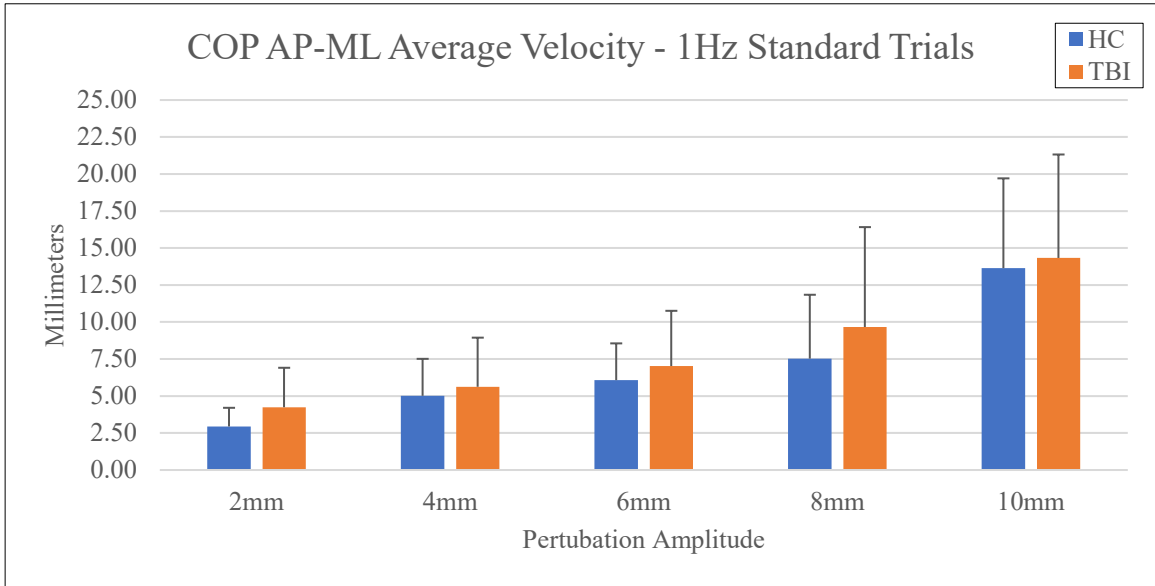


Figure 5.26. Mean AP-ML COP average velocity values for HC and TBI during perturbations delivered at 1.0Hz

The HC group’s mean AP COP range was larger for four out of the five perturbation amplitudes at 1.0Hz, while the TBI group’s mean was larger for the remaining perturbation. For the 10mm perturbation, the HC group’s mean was 10.62 ± 3.71 cm compared 8.58 ± 4.02 cm for the TBI group, and was 6.47 ± 2.35 cm vs 5.53 ± 3.48 cm for the 8mm perturbation. The HC group’s mean for the 6mm perturbation was 6.29 ± 1.39 cm compared to 4.45 ± 2.25 cm for the TBI group, and 4.99 ± 2.06 cm vs 4.00 ± 2.81 cm for the 4mm perturbation, respectively. For the 2mm perturbation, the TBI group’s mean was 2.97 ± 1.81 cm compared to 2.74 ± 0.87 cm for the HC group’s mean (Figure 3.27). Sphericity was not assumed for the AP COP range at 1.0Hz, though a significant within-subject effect of amplitude $[F(2.217,42.116) = 41.470, p < 0.001]$ was found after application of the Greenhouse-Geisser adjustment, not other effects were

significant (amplitude: $[F(2.217,42.116) = 1.338, p = 0.274]$, between-subject: $[F(1.000,19.000) = 1.317, p = 0.265]$).

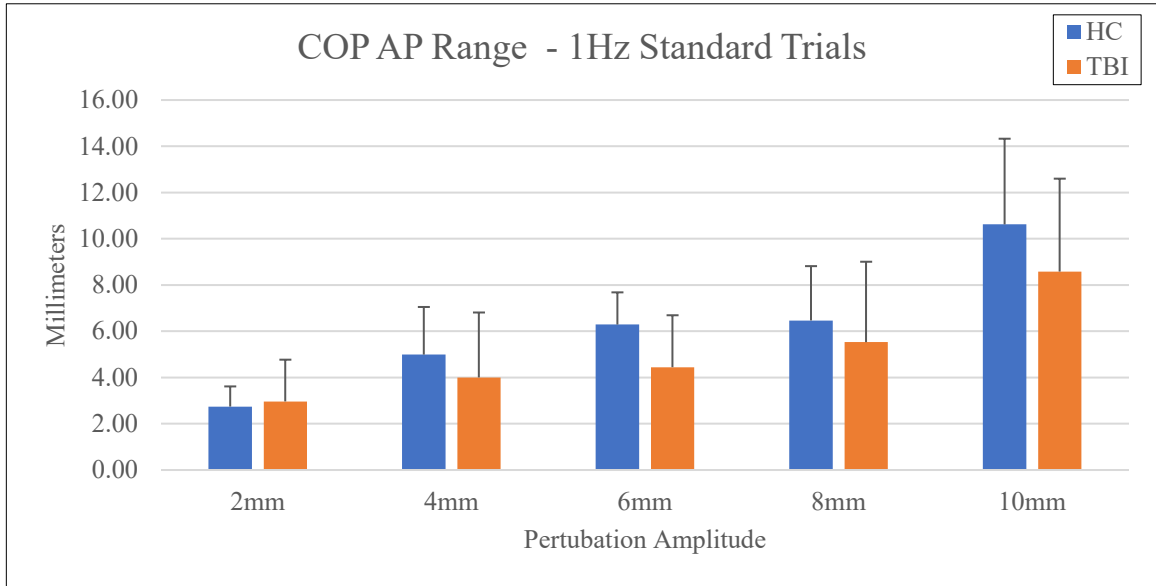


Figure 5.27. Mean AP COP range values for HC and TBI during perturbations delivered at 1.0Hz

5.4 Correlations Between Kinematic and Functional Measures

Scatter plots were generated for all possible combinations of frequency and amplitude for the hip and ankle joint ranges of motion vs each functional outcome measure (BBS, TUG, 5MWT, 10MWT) and the corresponding PPT (150 total), and correlations were run on each combination. However, out of all the correlations the largest R value was -0.7304, which corresponded to the range of motion about the ankle during the 10mm perturbation at 0.33Hz vs 0.33Hz PPT scores, and this correlation was only present for the HC group. A few other comparisons yielded similar R values, (1Hz_2mm_Hip_TUG_HC = -0.7210, and 033Hz_2mm_Ankle_BBS_HC = -0.6873), but these were also only for the HC group. The largest R values for the TBI group were

033Hz_6mm_Hip_BBS_TBI = -0.5616 and 033Hz_6mm_Ankle_BBS_TBI = -0.5532, with all other R values lower than ± 0.50 .

Linear regressions were performed for all correlations with an absolute value of R that was greater than 3.0, which left a total 59 correlations, 18 at 1Hz, 24 at 0.5Hz, and 17 at 0.33Hz. ANOVAs were then run on all the linear regressions to check for significance, yielding only three with $p < 0.5$. All three significant results were for HC comparisons, one was at 1Hz and the other two were at 0.33Hz. The significant 1Hz comparison was between the HCs range of motion about the hip for the 2mm perturbation vs. their TUG times [$F(1,7) = 7.5784, p = 0.0284, R^2 = 0.5198$]. One of the two comparisons at 0.33Hz also involved a functional measure, but in this case it was BBS scores vs. HCs range of motion about the ankle for the 2mm perturbation which was significant [$F(1,7) = 6.2682, p = 0.0408, R^2 = 0.4724$]. The final significant comparison at 0.33Hz was for the HCs range of motion about the ankle for the 10mm perturbation vs. their PPT scores at 0.33Hz [$F(1,7) = 8.0035, p = 0.0254, R^2 = 0.5334$].

CHAPTER 6

DISCUSSION

6.1 General Discussion

Substantial differences were noted between the TBI and HC groups for all functional measures, including a 7.35-point difference in the mean BBS scores, and the fact that the TBI group's mean completion times for the TUG, 5MWT, and 10 MWT were more than double the duration of the HC group's mean times. The TBI group's mean PPT for 0.33Hz and 1Hz were also more than double that of the HC group, while the difference was around 1.7x for the 0.5Hz PPT, but despite these differences, the only significant correlations were only found for three comparisons, two were between joint angle ranges of motion and functional measure scores for the HC group, and the third was between ankle range of motion and the 0.33Hz PPT for the HC group.

The first significant correlation was found between the HC group's hip range of motion for the 2mm perturbation at 1Hz and their TUG scores. As the TUG is a straightforward set of movements well within the range of normal everyday activities, it is expected that the HC group would have no difficulties with this task, and that their times for the task would generally tend to cluster together relatively close to the theoretical minimum amount of time needed to complete them, effectively resulting in a floor effect. The range of motion about the hip was very close to zero for the 2mm perturbation since the amplitude of the displacement was small, and this in turn likely resulted in a floor effect for the HC group leading to a significant correlation being found between the two very linear outcomes.

The second significant correlation was found for the HC group between their BBS scores and their range of motion about the ankle for the 2mm perturbation at 0.33Hz. Since the maximum score of the BBS is 56 and this score or very close to it was achieved by all HC participants, this resulted in a ceiling effect for the BBS scores. Owing to the very small and relatively slow perturbation delivered to the participant's base of support during the 2mm perturbation at 0.33Hz, it is fairly likely that the HC group's ankle ranges of motion were subjected to a floor effect of approaching the range of motion of standing unperturbed, once again leading to the significant correlation between two very linear measures.

The third significant correlation was found between ankle range of motion for the HC group for the 10mm perturbation at 0.33Hz and their 0.33Hz PPT scores. This negative relationship appears to indicate that the smaller the amplitude of perturbations that an individual is able to detect results in a larger ankle range of motion for those detected perturbations, which runs counter to expectations, as one would expect that an individual with sharper senses would be more stable, i.e. have a smaller range of motion about the ankle, than someone who is only able to detect larger perturbations. However, it is possible that the reason that the opposite is true in this case is that when an individual is able to detect even very small perturbations to their base of support, they are able to leverage that sensitivity to more efficiently modulate their postural responses to the perturbation and effectively "ride" the perturbation while only expending minimal effort to maintain their stability even over a larger range of motion, while someone who is less sensitive needs to make larger postural adjustments to compensate for their reduced ability to sense a given amplitude of perturbation and are therefore unable to "ride" the

perturbation as efficiently. Further investigation with more precise participant instructions will likely be necessary to further investigate this behavior.

Analysis of variance of the kinematic outcomes for the 0.33Hz perturbations found a significant within-subject effect of amplitude, which appears to validate that the difference between the perturbation amplitudes at 0.33Hz were sufficient to cause amplitude related responses from the participants for all kinematic measures except the hip, with no significant effect amplitude*group effect or between-subject effect. This result could represent the varying application of the pure ankle strategy over the amplitudes of the perturbations. For the 0.5Hz perturbations, a similar within-subject effect of amplitude was found for all kinematic outcomes except the ankle, COM path length, and COM average velocity, with once again no significant amplitude*group effect or between-subject effect. However, the lack of a within-subject effect of amplitude about the ankle is contrary to expectations as it is present in both the knee and hip. Significant within-subject effects of amplitude were found for all kinematic outcomes for the 1Hz perturbations which appears to validate that the difference between the perturbation amplitudes at 1.0Hz were sufficient to cause amplitude related responses from the participants for all kinematic measures, as expected, though the anticipated significant interaction effect of amplitude*group was not found. A significant between-subject effect about the ankle was found for the 6mm perturbation, but such an effect was expected to have included the 8 and 10mm perturbation amplitudes as well if any such effects were to be present. Overall, the anticipated differences between the perturbations had been expected to be more pronounced the higher the perturbation frequency, if they were

present at all for the lower frequency perturbation, especially for the lower amplitude perturbations, but these differences were not clearly visible in the current data.

6.2 Limitations

While the results of this study do show some promise that could serve to encourage further work in their area, the present study has several limitations that limit the application of the existing results. The primary limitations that affected the study were the small number of subjects whose data was usable for analysis, and the small number of trials run for each condition. The very large difference between the HC and TBI groups for the 10mm perturbations is likely at least partially a result of a startle/surprise factor since the 10mm was the first perturbation presented and was likely more substantial than most participants were expecting it to be. Additionally, several trials throughout the study had to be excluded from the analysis due to excess movements on the part of the participants since the criterion for when a trial should be repeated was not clearly established. Finally, participants did not undergo any range of motion testing as part of this study, making it more difficult to ascertain if the differences in the participants' movement patterns in response to the perturbations were the result of range of motion limitations or other factors.

6.3 Future Directions

In order to further improve upon the current study and increase the potential usefulness of its findings, additional studies need to be performed that take into account the lessons learned at present. A larger sample size will be needed in order to ensure that any outcomes have sufficient power to be statistically relevant, and several repetitions of each

perturbation at each frequency will need to be performed to reduce the likelihood of any startle responses and provide enough trials to enable the mean for each subject to properly characterize their response to the perturbations. To further eliminate the possibility of participants being startled by the platform movements, prior to the initiation of any data collection using the instrumented platform, every participant needs to be exposed to the full range of intensity of perturbations and types that will be encountered during the session, though whether these initial exposure trials should be presented as a single monolithic group at the beginning of the session or whether each type of perturbation and its associated range of intensities should be presented right before the start of real trials will need to be determined via additional testing.

To improve the quality and clinical relevance of the kinematic outcomes of future studies, the active and passive range of motion of all participants should be obtained prior to the start of any experimental procedures. This individual functional range of motion can be used to better understand the relative contributions of the multiple factors that can cause the use of particular balance control strategies for a given situation, including the useable range of movement of each joint, the available strength in the relevant muscle that need to be recruited for movements of the joints, the neurological control of the muscles involved, and movement planning of the central nervous system. Such information has the potential to be invaluable for determining the best approach to pursue to improve functional balance on an individual basis, and could enable clinicians to refer patients to whichever rehabilitation interventions are most likely to produce the largest functional result, be it stretching and strengthening, sensory practice, or particular balance training regimens.

If such evidence can be established with future applications of this research, then there exists significant potential to improve clinical assessments of balance dysfunction that are not subject to the limitations of current assessments such as the Berg Balance Scale which does not really assess functional balance and is unable to differentiate between different underlying sources of dysfunction, such as biomechanical or neurological sources. Placing an individual on the balance platform and affixing the necessary motion capture markers to enable the monitoring of their kinematics during an assessment, and performing the assessment, should not take much more than performing the BSS, and while it would require specialized equipment, many rehabilitation facilities already have balance platforms, and the overall technical setup of the system would be minimal once a procedure can be standardized from the applied research methods.

REFERENCES

- [1] “Get the Facts About TBI.” https://www.cdc.gov/traumaticbraininjury/get_the_facts.html (accessed Jan. 15, 2021).
- [2] “Types of Traumatic Brain Injury.” <https://www.brainline.org/article/types-traumatic-brain-injury> (accessed Jan. 15, 2021).
- [3] “Traumatic Brain Injury in the United States - Emergency Department Visits, Hospitalizations and Deaths 2002-2006 CDC,” 2006. [Online]. Available: <https://stacks.cdc.gov/view/cdc/5571> (accessed Sep. 13, 2022).
- [4] Management of Concussion/mTBI Working Group, “VA/DoD Clinical Practice Guideline for Management of Concussion/Mild Traumatic Brain Injury.,” *Journal of rehabilitation research and development*, vol. 46, no. 6, pp. CP1-68, 2009.
- [5] Peter Leo and Michael McCrea, *Epidemiology*. Boca Raton (FL): CRC Press/Taylor and Francis Group, 2016. doi: <https://www.ncbi.nlm.nih.gov/books/NBK326725/>.
- [6] “What Impact While Moderate or Severe TBI Have on a Person’s Life.” <https://www.brainline.org/article/what-impact-will-moderate-or-severe-tbi-have-persons-life> (accessed Jan. 15, 2021).
- [7] “Balance Problems After Traumatic Brain Injury.” <https://www.brainline.org/article/balance-problems-after-traumatic-brain-injury> (accessed Jan. 15, 2021).
- [8] R. J. Peterka, C. F. Murchison, L. Parrington, P. C. Fino, and L. A. King, “Implementation of a Central Sensorimotor Integration Test for Characterization of Human Balance Control During Stance,” *Frontiers in Neurology*, vol. 9, no. December 2018, doi: 10.3389/fneur.2018.01045.
- [9] L. M. Nashner and G. McCollum, “The organization of human postural movements: A formal basis and experimental synthesis,” *Behavioral and Brain Sciences*, vol. 8, no. 1, pp. 135–150, Mar. 1985, doi: 10.1017/S0140525X00020008.
- [10] L. Sherwood, *Human Physiology from cells to systems*, Seventh Ed. Belmont, CA: Brooks Cole, 2009.
- [11] Purves D, Augustine GJ, Fitzpatrick D, et al., editors., “Neuroscience,” 2nd edition. Sunderland, MA: Sinauer Associates, 2001. [Online]. Available: <https://www.ncbi.nlm.nih.gov/books/NBK10792/> (accessed Dec. 25, 2022).

- [12] K. P. Blum, C. Versteeg, J. Sombeck, R. H. Chowdhury, and L. E. Miller, “Chapter 2 - Proprioception: a sense to facilitate action,” in *Somatosensory Feedback for Neuroprosthetics*, Elsevier, 2021, pp. 41–76. doi: 10.1016/B978-0-12-822828-9.00017-4.
- [13] F. B. Horak and L. M. Nashner, “Central programming of postural movements: Adaptation to altered support-surface configurations,” *Journal of Neurophysiology*, vol. 55, no. 6, pp. 1369–1381, 1986, doi: 10.1152/jn.1986.55.6.1369.
- [14] L. M. Nashner, C. L. Shupert, F. B. Horak, and F. O. Black, “Organization of posture controls: An analysis of sensory and mechanical constraints,” *Progress in Brain Research*, vol. 80, no. C, pp. 411–418, 1989, doi: 10.1016/S0079-6123(08)62237-2.
- [15] D. Winter, “Human balance and posture control during standing and walking,” *Gait & Posture*, vol. 3, no. 4, pp. 193–214, Dec. 1995, doi: 10.1016/0966-6362(96)82849-9.
- [16] G. M. Blenkinsop, M. T. G. Pain, and M. J. Hiley, “Balance control strategies during perturbed and unperturbed balance in standing and handstand,” *Royal Society Open Science*, vol. 4, no. 7, 2017, doi: 10.1098/rsos.161018.
- [17] N. Gusi, J. Carmelo Adsuar, H. Corzo, B. del Pozo-Cruz, P. R. Olivares, and J. A. Parraca, “Balance training reduces fear of falling and improves dynamic balance and isometric strength in institutionalised older people: A randomised trial,” *Journal of Physiotherapy*, vol. 58, no. 2, pp. 97–104, 2012, doi: 10.1016/S1836-9553(12)70089-9.
- [18] Centers for Disease Control and Prevention, “Older Adult Fall Prevention - Facts About Falls,” 2021. [Online]. Available: <https://www.cdc.gov/falls/index.html> (accessed Oct. 27, 2022).
- [19] Centers for Disease Control and Prevention - National Center for Injury Prevention and Control, “Web-based Injury Statistics Query and Reporting System (WISQARS)” [Online]. Available: <http://www.cdc.gov/injury/wisqars> (accessed Nov. 15, 2022).
- [20] T. Paillard and F. Noé, “Techniques and Methods for Testing the Postural Function in Healthy and Pathological Subjects,” *BioMed Research International*, vol. 2015, 2015, doi: 10.1155/2015/891390.
- [21] D. C. Bland, C. Zampieri, and D. L. Damiano, “Effectiveness of physical therapy for improving gait and balance in individuals with traumatic brain injury: A systematic review,” *Brain Injury*, vol. 25, no. 7–8, pp. 664–679, Jul. 2011, doi: 10.3109/02699052.2011.576306.

- [22] R. Pilkar, K. K. Karunakaran, A. Veerubhotla, N. Ehrenberg, O. Ibrinke, and K. J. Nolan, "Evaluating Sensory Acuity as a Marker of Balance Dysfunction After a Traumatic Brain Injury: A Psychophysical Approach," *Frontiers in Neuroscience*, vol. 14, Aug. 2020, doi: 10.3389/fnins.2020.00836.
- [23] G. P. Williams, A. G. Schache, and M. E. Morris, "Mobility after traumatic brain injury: Relationships with ankle joint power generation and motor skill level," *The Journal of Head Trauma Rehabilitation*, vol. 28, no. 5, pp. 371–378, 2013, doi: 10.1097/HTR.0b013e31824a1d40.
- [24] G. Torres-Oviedo and L. H. Ting, "Muscle synergies characterizing human postural responses," *Journal of Neurophysiology*, vol. 98, no. 4, pp. 2144–2156, 2007, doi: 10.1152/jn.01360.2006.
- [25] S. A. Chvatal and L. H. Ting, "Common muscle synergies for balance and walking," *Frontiers in Computational Neuroscience*, vol. 7, no. Apr. 2013, pp. 1–14, 2013, doi: 10.3389/fncom.2013.00048.
- [26] L. H. Ting, "Dimensional reduction in sensorimotor systems: A framework for Understanding Muscle Coordination of Posture," *Progress in Brain Research* vol. 165 (2007): 299-321. doi:10.1016/S0079-6123(06)65019-X.
- [27] P. Konrad, *The ABC of EMG A Practical Introduction to Kinesiological Electromyography*, 1.4. 2006. [Online]. Available: <https://www.noraxon.com/wp-content/uploads/2014/12/ABC-EMG-ISBN.pdf> (accessed Oct. 27, 2022).
- [28] S. Al-Qaisi and F. Aghazadeh, "Electromyography Analysis: Comparison of Maximum Voluntary Contraction Methods for Anterior Deltoid and Trapezius Muscles," *Procedia Manufacturing*, vol. 3, (2015): 4578–4583. doi: 10.1016/j.promfg.2015.07.475.
- [29] N. Ehrenberg, A. Veerubhotla, K. Nolan, and R. Pilkar, "Balance Control Strategies during Perturbed Standing after a Traumatic Brain Injury: Kinematic Analysis," in *2021 43rd Annual International Conference of the IEEE Engineering in Medicine and Biology Society (EMBC)*, IEEE, Nov. 2021, pp. 4855–4858. doi: 10.1109/EMBC46164.2021.9630258.
- [30] R. Pilkar, K. K. Karunakaran, A. Veerubhotla, N. Ehrenberg, O. Ibrinke, and K. J. Nolan, "Evaluating Sensory Acuity as a Marker of Balance Dysfunction After a Traumatic Brain Injury: A Psychophysical Approach," *Frontiers in Neuroscience*, vol. 14, Aug. 2020, doi: 10.3389/fnins.2020.00836.
- [31] M. Campbell and A. Parry, "Balance disorder and traumatic brain injury: Preliminary findings of a multi-factorial observational study," *Brain Injury*, vol. 19, no. 13, pp. 1095–1104, 2005, doi: 10.1080/02699050500188898.

- [32] J. J. Sosnoff, S. P. Broglio, S. Shin, and M. S. Ferrara, "Previous mild traumatic brain injury and postural-control dynamics," *Journal of Athletic Training*, vol. 46, no. 1, pp. 85–91, 2011, doi: 10.4085/1062-6050-46.1.85.